

Geometric low-rank approximation of the Zeitlin model of incompressible fluids on the sphere

Cecilia Pagliantini*

Abstract

We consider the vorticity formulation of the Euler equations describing the flow of a two-dimensional incompressible ideal fluid on the sphere. Zeitlin’s model provides a finite-dimensional approximation of the vorticity formulation that preserves the underlying geometric structure: it consists of an isospectral Lie–Poisson flow on the Lie algebra of skew-Hermitian matrices. We propose an approximation of Zeitlin’s model based on a time-dependent low-rank factorization of the vorticity matrix and evolve a basis of eigenvectors according to the Euler equations. In particular, we show that the approximate flow remains isospectral and Lie–Poisson and that the error in the solution, in the approximation of the Hamiltonian and of the Casimir functions only depends on the approximation of the vorticity matrix at the initial time. The computational complexity of solving the approximate model is shown to scale quadratically with the order of the vorticity matrix and linearly if a further approximation of the stream function is introduced.

1 Introduction

The motion of inviscid ideal fluids is governed by the Euler equations which, for incompressible flows, read:

$$\begin{cases} \partial_t \mathbf{u} + \operatorname{div}(\mathbf{u} \otimes \mathbf{u}) + \nabla p = 0, \\ \operatorname{div} \mathbf{u} = 0, \end{cases} \quad (1.1)$$

where \mathbf{u} represents the velocity of the fluid, and p is the hydrodynamic pressure. In his pioneering work, Arnold [1] showed that ideal fluid motions describe geodesics on the Lie group of volume-preserving diffeomorphisms endowed with a right-invariant metric corresponding to kinetic energy. This result has not only brought to light the geometric structure underlying Euler’s equations but it has been used to give rigorous local well-posedness results [10], and to relate the stability of the fluid motion to the sectional curvature of the Riemannian metric. In addition to the incompressible Euler equations (1.1), many partial differential equations has been shown to fit the framework of Arnold, although for different infinite-dimensional groups and Riemannian metrics. These models are referred to as *Euler–Arnold equations* and include the Korteweg–de Vries equation, the Camassa–Holm equation, the Landau–Lifschitz equation, the magnetohydrodynamic equations, etc.

When looking at finite-dimensional approximations of the Euler equations, the traditional approach of considering the dynamical variables by Fourier transforming the system, and then truncating at some frequency hinders the geometric structure of the problem, see e.g. [21], and leads to unphysical numerical simulations. To retain as much as possible of the geometric structure of the Euler equations to the finite-dimensional approximation, numerical methods have been derived in several works [9, 30, 16, 17].

In this work we focus on the two-dimensional incompressible Euler equations on the sphere, relevant for geophysical flows, and leverage the finite-dimensional approximation introduced by Zeitlin [33, 32]. The Zeitlin model is, to the best of our knowledge, the only (spatial) finite-dimensional approximation of the two-dimensional Euler equations, on the torus and on the sphere, that fully adopts Arnold’s geometric description. The Zeitlin model consists of an isospectral Lie–Poisson flow for the vorticity matrix on the Lie algebra of skew-Hermitian $N \times N$ matrices. Local convergence of the solutions of the Zeitlin model to the solutions of the Euler equations, as $N \rightarrow \infty$, was first

*Dipartimento di Matematica, Università di Pisa, Pisa, Italy. (cecilia.pagliantini@unipi.it).

Funding from the MIUR Excellence Department Project awarded to the Department of Mathematics, University of Pisa, CUP I57G22000700001, and from the INDAM/GNCS 2024 project CUP E53C23001670001 are acknowledged.

established by Gallagher [15] and more recently in [12, 27]. Furthermore, it has been shown in [23] that the Zeitlin model also preserves the stable/unstable nature of stationary solutions of the Euler equations.

The fact that the Zeitlin model retains the geometric structure of the Euler equations – in the sense that it also describes geodesics on a Lie group with a right-invariant Riemannian metric – results in a coherent approach to the simulation of the qualitative long-time behavior of 2D Euler equations, as it has been recently discovered by Modin and co-authors [25, 26, 8]. In particular, numerical simulations based on Zeitlin’s model have been shown to reproduce the spectral power laws in the inverse energy cascade [7] and to ensure conservation of Casimir invariants, such as enstrophy, which is critical for 2D turbulence. The bulk of numerical simulations based on Zeitlin’s model rely on a family of numerical time integration schemes, introduced in [24], that preserve the isospectrality and Lie–Poisson structure of the flow. A major bottleneck of this family of time integrators is their computational complexity: the most used second order time integrator of this family scales as N^3 , even when an efficient computation of the stream function is considered [8].

In this work we propose a numerical approximation of the Zeitlin model that preserves the geometric structure of the problem, as derived by Arnold, at a favorable computational complexity. The idea is to perform a time-dependent low-rank factorization of the vorticity matrix and evolve a basis of eigenvectors according to the Euler equations. In particular, we show that the approximate flow remains isospectral and Lie–Poisson and that the error in the approximation of the Hamiltonian and of the Casimir functions only depends on the approximation of the vorticity matrix at the initial time. Moreover, we establish a priori error estimates showing that the error, in the Frobenius norm, between the solution of the Zeitlin model and the proposed low-rank approximation is bounded by the truncated singular values of the initial vorticity matrix. The computational complexity of solving the approximate model is shown to scale quadratically with N and linearly if a further approximation of the stream function is introduced. The proposed method has superior properties in terms of efficiency and accuracy whenever the dynamics has a low-rank structure, for example in the presence of point vortices. If this is not the case and the rank of the vorticity matrix equals N , then the proposed method provides an isospectral Lie–Poisson time integration scheme whose performances are comparable to solving the Zeitlin model with the numerical method of [24].

We also propose an extension of the low-rank approximation to general Euler–Arnold equations characterized by a non-isospectral flow. For this alternative approach, a structure-preserving time splitting is introduced to solve the evolution equations for the low-rank factors.

The remainder of the paper is organized as follows. In Section 2 we recall the Zeitlin truncation of the incompressible Euler equations on the sphere and summarize the second order isospectral Lie–Poisson time integrator proposed in [24]. Section 3 pertains to the derivation of a low-rank approximation of the Zeitlin model and to the discussion of its geometric properties and convergence results. The resulting approximate dynamics is solved by evolving a basis of eigenvectors, as described in Section 4, where a time discretization on the manifold of unitary matrices is presented. In Section 5 a truncation of the stream matrix is analyzed with the aim of further reducing the computational complexity of the approximate model. The extension to general Euler–Arnold equations with a factorization of the vorticity matrix with time-dependent factors is introduced in Section 6. Numerical experiments are discussed in Section 7. Section 8 presents some concluding remarks.

2 Vorticity formulation of incompressible Euler’s equations

Let $\mathcal{I} := (0, T] \subset \mathbb{R}$ be a given temporal interval, with $T \in \mathbb{R}$. We consider as spatial domain the unit sphere $\mathbb{S}^2 \subset \mathbb{R}^3$. Let $\omega : \mathcal{I} \times \mathbb{S}^2 \rightarrow \mathbb{R}$ be the vorticity defined as $\omega = \text{curl } \mathbf{u} = \text{sdiv } \mathbf{u}$ where $\text{sdiv}(\mathbf{u}_1, \mathbf{u}_2) := -\partial_y \mathbf{u}_1 + \partial_x \mathbf{u}_2$ is the skew-divergence. Problem (1.1) in the vorticity variable reads $\partial_t \omega = -\mathbf{u} \cdot \text{grad } \omega$. Introducing the stream function $\psi : \mathcal{I} \times \mathbb{S}^2 \rightarrow \mathbb{R}$ defined as $\text{curl } \psi = \text{sgrad } \psi = \mathbf{u}$, with the skew-gradient defined as $\text{sgrad } \psi := (-\partial_y \psi, \partial_x \psi)$, then the vorticity satisfies

$$\begin{cases} \partial_t \omega = -\text{grad } \omega \cdot \text{curl } \psi = -\{\psi, \omega\} & \text{in } \mathcal{I} \times \mathbb{S}^2, \\ \Delta \psi = \omega & \text{in } \mathcal{I} \times \mathbb{S}^2, \end{cases} \quad (2.1)$$

where the stream function ψ is related to the vorticity via the Laplace–Beltrami operator Δ , and $\{\cdot, \cdot\}$ is the Poisson bracket on \mathbb{S}^2 defined, for any $f, g \in C^\infty(\mathbb{S}^2)$, as

$$\{f, g\}(\mathbf{x}) = (\nabla f \times \nabla g)(\mathbf{x}), \quad \forall \mathbf{x} \in \mathbb{S}^2 \subset \mathbb{R}^3.$$

The configuration space of an ideal incompressible fluid filling \mathbb{S}^2 is the infinite-dimensional Lie group $G = \text{SDiff}(\mathbb{S}^2)$ of volume-preserving diffeomorphisms. The Lie algebra of G is formed by divergence-free vector fields on \mathbb{S}^2 with Lie bracket given by minus the Poisson bracket of vector fields. Hence, problem (2.1) is an infinite-dimensional Lie–Poisson system [2] on the space of smooth zero-mean functions

$$C_0^\infty(\mathbb{S}^2) = \left\{ \omega \in C^\infty(\mathbb{S}^2) : \int_{\mathbb{S}^2} \omega \, dx = 0 \right\}.$$

The Hamiltonian of the system is given by the kinetic energy

$$H(\omega) = \frac{1}{2} \int_{\mathbb{S}^2} \mathbf{u}^2 \, dx = -\frac{1}{2} \int_{\mathbb{S}^2} \psi \omega \, dx.$$

The Poisson tensor is $J = \text{grad } \omega \cdot \text{sgrad}$ and the variational derivative of the Hamiltonian is $\delta H = -\psi$. System (2.1) has an infinite number of Casimir invariants

$$\mathcal{C}_f(\omega) = \int_{\mathbb{S}^2} f(\omega) \, dx \quad \forall f \in C^\infty(\mathbb{R}).$$

Linear, quadratic, etc. invariants are obtained by taking $f(\omega)$ as monomials. Since the Casimir functions are conserved for any choice of the Hamiltonian, the system is characterized by a Lie–Poisson geometry foliated in co-adjoint orbits preserved by any Hamiltonian flow. The presence of these integrals imposes an infinite number of constraints on the dynamical variables given by the Fourier components of the vorticity field [33]. A crude truncation in Fourier space would hinder the geometric structure of the problem yielding an inconsistent approximation of the dynamics which induces, in turn, spurious effects and poorly accurate solutions. This problem was solved by Zeitlin [33, 32] via the so-called sine truncation and based on quantization results of Hoppe [19]. The idea is to generate a sequence of finite-mode approximations preserving the symplectic structure and providing a number of Casimir functions which tend to original ones when the truncation size N tends to infinity.

2.1 The Zeitlin model

The space $C_0^\infty(\mathbb{S}^2)$ of zero-mean real smooth functions over \mathbb{S}^2 endowed with the Poisson structure $\{\cdot, \cdot\}$ forms an infinite-dimensional Lie algebra. A finite-dimensional approximation of $(C_0^\infty(\mathbb{S}^2), \{\cdot, \cdot\})$ can be derived via L_α -approximation [4, Definition 2.1]. The idea is to construct a sequence of labeled Lie algebras whose limit is the given Lie algebra, see [4] for further details on L_α -limits.

On the sphere \mathbb{S}^2 , an approximating sequence for $(C_0^\infty(\mathbb{S}^2), \{\cdot, \cdot\})$ was constructed in [20, 3, 4] via the family of Lie algebras $(\mathfrak{u}(N), [\cdot, \cdot]_N)_{N \in \mathbb{N}}$ where $[\cdot, \cdot]_N := \frac{1}{2}(N^2 - 1)^{1/2}[\cdot, \cdot]$ is a suitable rescaling of the matrix commutator, see [27, Section 3.1] for a detailed derivation. The information that relates the approximating sequence and the limit algebra is encoded in surjective projection operators $\{p_N\}_{N \in \mathbb{N}}$. Let us consider the $L^2(\mathbb{S}^2)$ -orthogonal basis for $C_0^\infty(\mathbb{S}^2)$ provided by the complex spherical harmonics, which, in azimuthal-inclination coordinates, are defined as

$$Y_{\ell, m}(\Phi, \theta) = \sqrt{\frac{2\ell + 1}{4\pi} \frac{(\ell - m)!}{(\ell + m)!}} P_\ell^m(\cos(\theta)) e^{im\Phi}, \quad \ell \geq 1, -\ell \leq m \leq \ell,$$

where $\{P_\ell^m\}_{\ell, m}$ are the associated Legendre polynomials. The projections $p_N : C_0^\infty(\mathbb{S}^2) \rightarrow \mathfrak{u}(N)$ can then be defined as

$$\omega(\Phi, \theta) = \sum_{\ell=1}^{\infty} \sum_{m=-\ell}^{\ell} \omega^{\ell m} Y_{\ell, m}(\Phi, \theta) \mapsto \sum_{\ell=1}^{N-1} \sum_{m=-\ell}^{\ell} i\omega^{\ell m} T_{\ell, m}^N = W,$$

by associating to each spherical harmonic $Y_{\ell, m}$ a matrix $T_{\ell, m}^N \in \mathfrak{sl}(N, \mathbb{C})$ defined as

$$(T_{\ell, m}^N)_{m_1, m_2} := (-1)^{s-m_1} \sqrt{2\ell + 1} \begin{pmatrix} s & \ell & s \\ -m_1 & m & m_2 \end{pmatrix}, \quad s := \frac{N-1}{2}$$

where the term in brackets denotes the Wigner 3j-symbol. Note that $T_{\ell, m}^N$, for any fixed pair (ℓ, m) , has non-zero entries only on the $-m$ th diagonal. Indeed, by the properties of the Wigner 3j-symbol,

$(T_{\ell,m}^N)_{m_1,m_2} = 0$ whenever $-m_1 + m + m_2 \neq 0$. Moreover, the matrices $\{T_{\ell,m}^N\}_{\ell,m}$ are orthogonal with respect to the Frobenius inner product $\langle \cdot, \cdot \rangle$, which corresponds to the fact that the spherical harmonics $\{Y_{\ell,m}\}_{\ell,m}$ are orthogonal with respect to the inner product in $L^2(\mathbb{S}^2)$.

It has been proven in [4] that, for the projections p_N defined above and any choice of the matrix norm d_N , the family of finite-dimensional Lie algebras $(\mathfrak{u}(N), [\cdot, \cdot]_N)_{N \in \mathbb{N}}$ is an L_α -approximation of $(C_0^\infty(\mathbb{S}^2), \{\cdot, \cdot\})$. Therefore, the truncation introduced by Zeitlin [33] provides a finite-dimensional approximation of the incompressible Euler equations (2.1) that preserves the Hamiltonian structure and the conservation laws and reads as follows: given $W(0) = W_0 \in \mathfrak{u}(N)$, find $W \in C^1(0, T; \mathfrak{u}(N))$ such that

$$\begin{cases} \dot{W} = [P(W), W], \\ \Delta_N P = W, \end{cases} \quad (2.2)$$

where Δ_N is a discrete Laplacian that, however, is not uniquely defined. Typically, the discrete Laplacian is taken so that it keeps the spectral properties of the Laplace operator [20]:

$$\Delta_N^{-1} T_{\ell,m}^N = -\frac{1}{\ell(\ell+1)} T_{\ell,m}^N, \quad 1 \leq \ell \leq N-1, \quad -\ell \leq m \leq \ell, \quad (2.3)$$

meaning that $T_{\ell,m}^N$ is eigenvector of Δ_N with eigenvalue $-\ell(\ell+1)$. The operator Δ_N^{-1} is normal since it has a basis of eigenvectors that are orthogonal in the Frobenius norm, and it is symmetric since its eigenvalues are real. Hence, Δ_N^{-1} is self-adjoint with respect to the Frobenius inner product.

For an efficient computation of the inverse discrete Laplacian one can observe, as in [8], that Δ_N is a fourth order tensor which can be split into $2N-1$ blocks $\{\Delta^m\}_{m=-(N-1)}^{N-1}$ of size $N-|m|$, for $m = -(N-1), \dots, N-1$. Then, the computation of the potential matrix P consists in solving a linear system for each Δ^m with right hand side given by the m th diagonal of W and giving the m th diagonal of P . Each Δ^m , for $m \geq 0$, is a tridiagonal symmetric matrix of size $N-|m|$, defined as in [8, Equation (13)], namely, for $j = 1, \dots, N-m$,

$$\begin{aligned} (\Delta^m)_{j,j} &= 2(s(2j-1+m) - (j-1)(j-1+m)), \\ (\Delta^m)_{j,j+1} &= -\sqrt{(j+m)(N-j-m)j(N-j)} \\ (\Delta^m)_{j,j-1} &= -\sqrt{(j-1+m)(N-j+1-m)(j-1)(N-j+1)} \end{aligned}$$

and $\Delta^{-|m|} = \Delta^{|m|}$ for any m .

In the next result we collect the geometric properties of problem (2.2).

Lemma 2.1. *The finite-dimensional system (2.2) is Lie-Poisson on the dual of $\mathfrak{u}(N)$: it can be written as*

$$\dot{W} = [\nabla H(W), W] = J(W) \nabla H(W),$$

where the Poisson operator J is defined as $J(W)X = [X, W]$ for any $X \in \mathbb{C}^{N \times N}$, and the Hamiltonian is

$$H(W) = \frac{1}{2} \text{Tr}(P(W)W^*). \quad (2.4)$$

Moreover, the flow of (2.2) is isospectral and the quantities

$$C_k(W) := \text{Tr}(W^k), \quad k = 1, \dots, N, \quad (2.5)$$

are Casimir invariants.

Proof. Owing to the fact that the (inverse) Laplacian is self-adjoint with respect to the Frobenius inner product, it can be easily shown that $\nabla H(W) = P(W)$.

To show that the flow of system (2.2) is isospectral one can proceed as in, e. g., [18, Section IV.3.2]. Let $R : t \rightarrow \mathbb{C}^{N \times N}$ be solution of $\dot{R} = P(W(t))R$ with initial condition $R(t_0) = I$. Since P is skew-Hermitian, $R(t)$ is unitary for all $t \geq t_0$. This can be proven by simply showing that $I(R) := R^*R$ is an invariant of motion. Then, $\dot{R} = d_t(RRR^{-1}) = \dot{R} + R\dot{R}R^{-1} + RRd_t(R^{-1})$. Hence, $d_t(R^{-1}) = -R^{-1}P(W)$. Using this property and the evolution equation for R results in

$$d_t(R^{-1}WR) = R^{-1}(\dot{W} - [P(W), W])R = 0.$$

This implies that $R^{-1}(t)W(t)R(t) = R_0^{-1}W_0R_0 = W_0$ for all $t \geq t_0$. Hence $W(t) = R(t)W_0R^{-1}(t)$ is the solution of (2.2) for any $t > 0$, and the eigenvalues are preserved since $R(t)$ is unitary.

To show that the functions C_k , for $1 \leq k \leq N$, are Casimirs, we verify that

$$\{f, C_k\}(W) := \langle J(W)\nabla f(W), \nabla C_k(W) \rangle = 0 \quad \forall W \in \mathfrak{u}(N), f \in C^\infty.$$

Let $k = 1, \dots, N$ be fixed. Then,

$$\langle J(W)\nabla f(W), \nabla C_k(W) \rangle = k \langle [\nabla f(W), W], W^{k-1} \rangle = k \operatorname{Tr}(W^{k-1}\nabla f(W)W - W^k\nabla f(W)) = 0,$$

for any $W \in \mathfrak{u}(N)$ and smooth function f . \square

Remark 2.1. *The above result suggests that there exists a unitary $R \in \mathbb{C}^{N \times N}$ that satisfies $\dot{R} = P(RW_0R^{-1})R$ and such that $R(t)W_0R^{-1}(t)$ is the solution of (2.2). The approximation proposed in Section 4 is inspired by this consideration.*

Remark 2.2. *The Hamiltonian of (2.2) is a real quantity provided that W is full rank. Indeed, under this assumption, it can be shown that the eigenvalues of $P(W)W$ are either real or complex conjugate.*

2.2 Time integration of the Zeitlin model

Let us consider a uniform partition of the temporal interval $\mathcal{I} = (0, T] = \cup_\tau \mathcal{I}_\tau$ where $\mathcal{I}_\tau := (t_\tau, t_{\tau+1}]$, $t_\tau := \tau\Delta t$ with $0 \leq \tau \leq N_t - 1$ and $\Delta t = T/N_t$.

In [24] a numerical temporal integrator that preserves the Lie–Poisson and isospectral structure of the flow of (2.2) was introduced. In this section we recall a second order integrator from the family of methods introduced in [24], the one that has been mostly used in numerical simulations of the Zeitlin model and its extensions [8, 13, 14].

In each temporal subinterval \mathcal{I}_τ , with $\tau \geq 0$, given W_τ , the method consists in setting $\widetilde{W}^{(0)} = W_\tau$ and then computing

$$\widetilde{W}^{(j+1)} = W_\tau + \frac{\Delta t}{2}[P(\widetilde{W}^{(j)}), \widetilde{W}^{(j)}] + \frac{\Delta t^2}{4}P(\widetilde{W}^{(j)})\widetilde{W}^{(j)}P(\widetilde{W}^{(j)}), \quad j = 0, 1, \dots, \quad (2.6)$$

until a certain stopping criterion is satisfied. For example, one can check that the norm $\|\widetilde{W}^{(j+1)} - \widetilde{W}^{(0)}\|_\infty$ is below a given tolerance and the number of iterations does not exceed a given threshold. Once the update has stopped at the n_{it}^τ th iteration, one sets $\widetilde{W} = \widetilde{W}^{(n_{\text{it}}^\tau)}$ and compute the updated vorticity matrix as

$$W_{\tau+1} = \left(I + \frac{\Delta t}{2}P(\widetilde{W}) \right) \widetilde{W} \left(I - \frac{\Delta t}{2}P(\widetilde{W}) \right). \quad (2.7)$$

Note that, to the best of our knowledge, this is the lowest order time integrator of this family since it is not possible, with a similar approach, to construct a first order Lie–Poisson isospectral integrator on $\mathfrak{u}(N)$.

Proposition 2.1. *Let us consider the numerical time integration scheme (2.6)-(2.7) for the approximation of problem (2.2) over the temporal interval $\mathcal{I}_\tau = (t_\tau, t_{\tau+1}]$, $\tau \geq 0$. The arithmetic complexity of the algorithm is*

$$O(N^3 n_{\text{it}}^\tau)$$

where n_{it}^τ is the number of iterations required by the nonlinear step (2.6).

Proof. As shown in [8], the computation of the stream matrix can be performed in cN^2 operations, for some constant $c \in \mathbb{R}_+$. Indeed, as shown in Section 2, the stream matrix P satisfying the Laplacian problem in (2.2) can be obtained by solving N linear systems $\Delta^m p_m = w_m$ for $m = 0, \dots, N-1$, where p_m and w_m denote the m th diagonals of P and W , respectively. Since each system has size $N-m$ and it is tridiagonal, Thomas algorithm allows a linear cost in the dimension $N-m$.

Moreover, at the j th iteration of the nonlinear solver (2.6), the computation of the bracket requires one multiplication of the stream matrix and of the vorticity matrix, while the last term of (2.6) requires one further matrix-matrix multiplication. Hence, two (typically dense) matrix-matrix multiplications, of complexity $O(N^3)$, are needed for each update of $\widetilde{W}^{(j)}$ and W_τ , namely $n_{\text{it}}^\tau + 1$ times. More precisely, given the stream matrix $P(\widetilde{W}^{(j)})$, each iteration requires $4N^3 + N^2$ operations. Therefore, the total arithmetic complexity of the algorithm in \mathcal{I}_τ is $(n_{\text{it}}^\tau + 1)(4N^3 + (c+1)N^2)$ and the conclusion follows. \square

3 Geometric low-rank approximation of the Zeitlin model

We propose to approximate, for any $t \in \mathcal{I}$, $W(t) \in \mathfrak{u}(N)$ solution of (2.2) with a matrix-valued trajectory $Y(t)$ in the subspace $\mathcal{M}_r \cap \mathfrak{u}(N)$, where \mathcal{M}_r is the manifold of rank- r matrices

$$\mathcal{M}_r := \{A \in \mathbb{C}^{N \times N} : \text{rank}(A) = r \leq N\}.$$

Remark 3.1. *If W_0 has rank $r \leq N$, then the solution $W(t)$ of (2.2) belongs to \mathcal{M}_r at all times $t \in \mathcal{I}$ since the flow is isospectral. This means that the velocity field of the flow $X_H(W) := [P(W), W]$ belongs to the tangent space $T_W \mathcal{M}_r$ of \mathcal{M}_r at W .*

We aim at constructing an approximate trajectory $t \mapsto Y(t) \in \mathcal{M}_r$ with the following properties for any $t \in \mathcal{I}$: (i) the approximate trajectory remains on the Lie algebra, i.e. $Y(t) \in \mathfrak{u}(N)$; (ii) the flow of $Y(t)$ is Lie–Poisson on the dual of $\mathfrak{u}(N)$ and isospectral; (iii) $Y(t)$ is a good approximation of $W(t)$ in a sense to be defined; and (iv) $Y(t)$ is computationally less expensive to compute than $W(t)$. Note that we want these properties to hold both at the continuous level and after temporal discretization.

As observed in Remark 3.1, since the flow of (2.2) is isospectral, the velocity field X_H applied to any rank- r matrix Y belongs to $T_Y \mathcal{M}_r$. This means that approximating the evolution of Y with the flow whose velocity field is given by X_H corresponds to approximating the equation for W in (2.2) with its projection onto the tangent space of \mathcal{M}_r . Hence, the dynamical system for the low-rank approximate state reads: given $Y(0) = Y_0 \in \mathcal{M}_r \cap \mathfrak{u}(N)$, find $Y \in C^1(0, T; \mathcal{M}_r \cap \mathfrak{u}(N))$ such that

$$\begin{cases} \dot{Y} = [P(Y), Y], \\ \Delta_N P = Y, \end{cases} \quad (3.1)$$

where Y_0 is obtained by diagonalizing W_0 and truncating to the r largest eigenvalues. Let $\sigma_1(W_0) \geq \dots \geq \sigma_N(W_0)$ be the singular values of W_0 and let $\{\lambda_j(W_0)\}_{j=1}^N$ be the (purely imaginary) eigenvalues of W_0 ordered such that $|\lambda_1(W_0)| \geq \dots \geq |\lambda_N(W_0)|$. Note that $|\Im(\lambda_k(W_0))| = \sigma_k(W_0)$ for $1 \leq k \leq N$. The aforementioned choice of Y_0 gives $\sigma_k(Y_0) = \sigma_k(W_0)$ and $\lambda_k(Y_0) = \lambda_k(W_0)$ for all $1 \leq k \leq r$.

With such construction the solution of problem (3.1) retains the geometric structure of the original problem (2.2), as summarized in the next result.

Proposition 3.1. *The approximate dynamical system (3.1) is isospectral and Lie–Poisson on the dual of $\mathfrak{u}(N)$ with Hamiltonian given by (2.4), that is $H(Y) = \frac{1}{2} \text{Tr}(P(Y)Y^*)$.*

The proof of this result is analogous to the one of Lemma 2.1. It then follows that the functions (2.5) are Casimir invariants of (3.1). This, in turn, implies that the error between the k th Casimir evaluated at the exact solution W of (2.2) and at the approximate solution Y of (3.1) is given by

$$|C_k(W(t)) - C_k(Y(t))| = |C_k(W_0) - C_k(Y_0)| = |\text{Tr}(W_0^k) - \text{Tr}(Y_0^k)| = \left| \sum_{j=r+1}^N \lambda_j^k(W_0) \right|, \quad (3.2)$$

that is, it only depends on the approximation at the initial time. Similarly, the Hamiltonian satisfies

$$|H(W(t)) - H(Y(t))| = |H(W_0) - H(Y_0)|.$$

In the next section we analyze the accuracy of the proposed approximation.

3.1 A priori error estimates

In this section we derive an a priori bound on the error between the solution W of (2.2) and the solution Y of the approximate dynamics (3.1). To this end, we first prove the Lipschitz continuity of the velocity field of (2.2) in the Frobenius norm.

Lemma 3.1. *The operator $X_H : \mathfrak{u}(N) \rightarrow \mathfrak{u}(N)$ defined as $X_H(A) := [\Delta_N^{-1}A, A]$, for any $A \in \mathfrak{u}(N)$, is Lipschitz continuous in the Frobenius norm.*

Proof. Let $\mathcal{D} := \{\text{vec}(A) \in \mathbb{C}^{N^2} : A \in \mathfrak{u}(N)\} \subset \mathbb{C}^{N^2}$ and let $\psi : \mathcal{D} \rightarrow \mathcal{D}$ be defined as

$$\psi(\text{vec}(A)) = \text{vec}(X_H(A)) = -(I_N \otimes A - A^\top \otimes I_N) \text{vec}(\Delta_N^{-1}A), \quad \forall A \in \mathfrak{u}(N).$$

Since the inverse Laplace operator Δ_N^{-1} is a linear operator, there exists a matrix $L \in \mathbb{R}^{N^2 \times N^2}$ such that $\text{vec}(\Delta_N^{-1}A) = L \text{vec}(A)$. Let $J_\psi(\text{vec}(A)) \in \mathbb{C}^{N^2 \times N^2}$ denote the Jacobian matrix of ψ at $\text{vec}(A)$. We observe that $\psi \in C^1$ and the map $\text{vec}(A) \mapsto J_\psi(\text{vec}(A))$ is continuous. Since \mathcal{D} is compact, $\|J_\psi(\text{vec}(A))\|_2$ attains a maximum value in \mathcal{D} . \square

To derive a priori error estimates between the solution W of (2.2) and the solution Y of the approximate dynamics (3.1), we derive an error bound between Y and the best low-rank approximation of W at each time. Since the flow (2.2) is isospectral, the error between $W(t)$ and its best rank- r approximation $W^{\text{svd}}(t)$, which is given by the truncated SVD of $W(t)$ at time $t \in \mathcal{I}$, is constant in time: by Eckart–Young–Mirsky theorem [11], it holds

$$\|W(t) - W^{\text{svd}}(t)\|^2 = \sum_{i=r+1}^N \sigma_i^2(W_0).$$

Note that the best rank- r approximation is unique if and only if $\sigma_r(W(t)) \neq \sigma_{r+1}(W(t))$, for all t . Without loss of generality we can always consider the case in which r is such that $\sigma_r(W_0) > \sigma_{r+1}(W_0)$.

Observe that the best low-rank approximation W^{svd} of W satisfies the evolution equation

$$\dot{W}^{\text{svd}} = [P(W), W^{\text{svd}}] = X_H(W^{\text{svd}}) + [P(W - W^{\text{svd}}), W^{\text{svd}}] \quad (3.3)$$

where the first term only depends on the retained modes, while the last term takes into account the interaction of the retained modes with the neglected ones. To better highlight the relationship between the evolution of W^{svd} and the one of the approximate state Y from (3.1), equation (3.3) can be equivalently written as

$$\dot{W}^{\text{svd}} = \Pi_{T_{W^{\text{svd}}}\mathcal{M}_r}(X_H(W)) + L_{W^{\text{svd}}}[W - W^{\text{svd}}](X_H(W))$$

where $X \mapsto L_{W^{\text{svd}}}[N](X)$ is the Weingarten map at W^{svd} with normal direction N .

Proposition 3.2. *For any $t \in (0, T]$, let $Y(t)$ be the solution of (3.1) and let $W^{\text{svd}}(t)$ be the best rank- r approximation of $W(t)$, where $W(t)$ is solution of (2.2). Then,*

$$\|Y(t) - W^{\text{svd}}(t)\| \leq (1 + K^{-1}\|\Delta_N^{-1}\|_2\|W_0\|) (e^{Kt} - 1) \sqrt{\sum_{i=r+1}^N \sigma_i^2(W_0)}, \quad (3.4)$$

where K is the Lipschitz continuity constant of X_H .

Proof. Using the evolution equations (3.3) for W^{svd} and (3.1) for Y gives

$$\begin{aligned} \|\dot{Y}(t) - \dot{W}^{\text{svd}}(t)\| &= \|X_H(Y) - [P(W), W^{\text{svd}}]\| \\ &\leq \|X_H(W) - X_H(Y)\| + \|X_H(W) - [P(W), W^{\text{svd}}]\|. \end{aligned} \quad (3.5)$$

The first term can be bounded using the Lipschitz continuity of the Hamiltonian vector field X_H as shown in Lemma 3.1. This gives

$$\|X_H(W) - X_H(Y)\| \leq K\|W - W^{\text{svd}}\| + K\|Y - W^{\text{svd}}\|.$$

The second term in (3.5) can be bounded using the linearity of the commutator as

$$\|X_H(W) - [P(W), W^{\text{svd}}]\| \leq \|[P(W), W - W^{\text{svd}}]\| \leq \|P(W)\|\|W - W^{\text{svd}}\|.$$

Moreover, $\|P(W)\| \leq \|\Delta_N^{-1}\|_2\|W\| = \|\Delta_N^{-1}\|_2\|W_0\|$, for any $t \geq 0$. Note that, more generally, the norm of the velocity field of the flow satisfies [31, Theorem 2.2]

$$\|X_H(W)\|^2 = \|[P(W), W]\|^2 \leq 2\|P(W)\|^2\|W\|^2 - 8H(W)^2 \leq 2\|\Delta_N^{-1}\|_2^2\|W_0\|^4 - 8H(W)^2.$$

Combining the bounds above we get, for any $t \geq 0$

$$\|\dot{Y}(t) - \dot{W}^{\text{svd}}(t)\| \leq (K + \|\Delta_N^{-1}\|_2 \|W_0\|) \|W(t) - W^{\text{svd}}(t)\| + K \|W^{\text{svd}}(t) - Y(t)\|.$$

Using Gronwall's inequality and the fact that $\|W(t) - W^{\text{svd}}(t)\| = \|W_0 - W_0^{\text{svd}}\|$ yields

$$\|Y(t) - W^{\text{svd}}(t)\| \leq (K + \|\Delta_N^{-1}\|_2 \|W_0\|) \|W_0 - W_0^{\text{svd}}\| \int_0^t e^{K(t-s)} ds.$$

□

The proposed low-rank approximation preserves the geometric structure of the Zeitlin model and it converges to its solution in the sense of Proposition 3.2. However, solving the approximate problem (3.1) using the time integration scheme of Section 2.2 is as computationally expensive as solving the original problem (2.2). The idea is then to exploit the low-rank structure of the approximate solution Y via a suitable factorization. In the next sections we consider two possible options.

4 Fixed spectrum approximation

We want to efficiently solve the approximate dynamics (3.1) on the rank- r matrix manifold \mathcal{M}_r by exploiting a factorization of the state $Y(t)$ at any $t \in \mathcal{I}$. At the initial time, since W_0 is normal, it is unitarily diagonalizable, namely there exist D_0 diagonal and V_0 unitary such that $W_0 = V_0 D_0 V_0^*$. We then approximate the solution $W(t) \in \mathfrak{u}(N)$ of (2.2), at any time $t \in \mathcal{I}$, with

$$Y(t) = U(t) S_0 U^*(t) \quad \text{in } \mathcal{M}_r \cap \mathfrak{u}(N), \quad (4.1)$$

where $S_0 \in \mathbb{C}^{r \times r}$ contains the r largest eigenvalues of W_0 . At the initial time we set $U(t_0) = U_0 \in \mathbb{C}^{N \times r}$ where the columns of U_0 are the eigenvectors associated with the r largest eigenvalues of W_0 . Moreover, we require that, for any $t \in \mathcal{I}$, $U(t)$ belongs to the Stiefel manifold

$$\text{St}(r, \mathbb{C}^N) := \{M \in \mathbb{C}^{N \times r} : M^* M = I_r\}.$$

Under these hypotheses, the evolution equation for the matrix $Y(t)$ given in (3.1) can be written as

$$\dot{Y} = [P(Y), U S_0 U^*] = P(Y) U S_0 U^* - U S_0 U^* P(Y).$$

Since $\dot{Y} = \dot{U} S_0 U^* + U S_0 \dot{U}^*$, one gets the equation for the factor U on $\text{St}(r, \mathbb{C}^N)$,

$$\begin{cases} \dot{U} = P(U S_0 U^*) U, \\ U(t_0) = U_0 \in \text{St}(r, \mathbb{C}^N). \end{cases} \quad (4.2)$$

If the rank of the solution W of the original problem (2.2) is $r \leq N$, then the approximate state Y obtained from the solution of (4.2) coincides with W , as shown in the next result.

Proposition 4.1 (Exactness property). *Let $W(t)$ be the solution of problem (2.2) at time $t \in \mathcal{I}$ with initial condition W_0 having rank $r \leq N$. Let the eigendecomposition of W_0 be $W_0 = V_0 S_0 V_0^*$ with $V_0 \in \text{St}(r, \mathbb{C}^N)$ and $S_0 \in \mathbb{C}^{r \times r}$ containing the non-zero eigenvalues of W_0 . If $Y(t) = U(t) S_0 U^*(t)$ is such that $U(t) \in \mathbb{C}^{N \times r}$ is solution of (4.2) with $U(t_0) = V_0$ then $Y(t) = W(t)$ for any $t \geq t_0$.*

Proof. By the isospectrality of the flow, the solution $W(t)$ of (2.2), at any time $t \in \mathcal{I}$, can be written as $W(t) = R(t) W_0 R^*(t)$ where $R(t) \in \text{St}(N, \mathbb{C}^N)$ satisfies $\dot{R}(t) = P(W(t)) R(t)$ with $R(t_0) = I$, as shown in the proof of Lemma 2.1. Then, using the eigendecomposition of W_0 , results in $W(t) = R(t) V_0 S_0 V_0^* R^*(t)$. Let $V(t) := R(t) V_0 \in \text{St}(r, \mathbb{C}^N)$, for any $t \in \mathcal{I}$. This satisfies the equation

$$\begin{cases} \dot{V}(t) = \dot{R}(t) V_0 = P(V(t) S_0 V^*(t)) V(t), \\ V(t_0) = V_0 \in \text{St}(r, \mathbb{C}^N). \end{cases}$$

which coincides with problem (4.2) provided $U_0 = V_0$, or equivalently $Y(t_0) = W(t_0)$. □

Remark 4.1. *By construction, the approximate state $Y = U S_0 U^*$, obtained by solving (4.2) for U , satisfies the properties discussed in Section 3, in particular Proposition 3.1 and Proposition 3.2.*

For the numerical temporal approximation of problem (4.2) we need to make sure that $U(t) \in \mathbb{C}^{N \times r}$ remains unitary for all t . Moreover, we would like to achieve a computational complexity lower than the one required to solve the original problem (2.2) and described in Proposition 2.1.

4.1 Time integration of unitary flows

In this section we describe and analyze numerical time integrators for the solution of the evolution equation (4.2) based on Lie groups acting on manifolds.

Let us first observe that problem (4.2) can be written as $\dot{U}(t) = \mathcal{L}_{S_0}(U(t))U(t)$ for some $\mathcal{L}_{S_0} : \text{St}(r, \mathbb{C}^N) \rightarrow \mathfrak{u}(N)$. The idea is then to derive an evolution equation on the Lie algebra $\mathfrak{u}(N)$ via a coordinate map (of the first kind), namely a smooth function $\psi : \mathfrak{u}(N) \rightarrow \mathcal{U}(N)$ where $\mathcal{U}(N)$ denotes the unitary group. The coordinate map should satisfy $\psi(0) = I \in \mathcal{U}(N)$ and $d\psi_0 = I$, where $d\psi : \mathfrak{u}(N) \times \mathfrak{u}(N) \rightarrow \mathfrak{u}(N)$ is the right trivialized tangent of ψ defined as

$$\frac{d}{dt}\psi(A(t)) = d\psi_{A(t)}(\dot{A}(t))\psi(A(t)), \quad \forall A : \mathbb{R} \rightarrow \mathfrak{u}(N).$$

For sufficiently small $t \geq t_0$, the solution of (4.2) is given by $U(t) = \psi(\Omega(t))U(t_0)$ where $\Omega(t) \in \mathfrak{u}(N)$ satisfies

$$\dot{\Omega}(t) = d\psi_{\Omega(t)}^{-1}(\mathcal{L}_{S_0}(U(t))), \quad \text{for } t \in \mathcal{I}, \quad (4.3)$$

with $\Omega(t_0) = 0$. Problem (4.3) can be solved using traditional Runge–Kutta (RK) methods. Let $(b_i, a_{i,j})$, for $i = 1, \dots, N_s$ and $j = 1, \dots, N_s$, be the coefficients of the Butcher tableau describing an N_s -stage explicit RK method. Then, the numerical approximation of (4.3) in the interval $\mathcal{I}_\tau = (t_\tau, t_{\tau+1}]$, $\tau \geq 0$, is performed as in Algorithm 1. This approach falls within the class of numerical integration schemes known as Runge–Kutta Munthe-Kaas (RK-MK) methods [28].

Algorithm 1 Explicit RK-MK scheme to solve (4.3) in $(t_\tau, t_{\tau+1}]$

Input: $U_\tau \in \text{St}(r, \mathbb{R}^N)$, $\{b_i\}_{i=1}^{N_s}$, $\{a_{i,j}\}_{i,j=1}^{N_s}$

1: $\Omega_\tau^1 = 0$, $U_\tau^1 = U_\tau$

2: **for** $i = 2, \dots, N_s$ **do**

3: $\Omega_\tau^i = \Delta t \sum_{j=1}^{i-1} a_{i,j} d\psi_{\Omega_\tau^j}^{-1}(\mathcal{L}_{S_0}(U_\tau^j))$,

4: $U_\tau^i = \psi(\Omega_\tau^i)U_\tau$,

5: **end for**

6: $\Omega_{\tau+1} = \Delta t \sum_{i=1}^{N_s} b_i d\psi_{\Omega_\tau^i}^{-1}(\mathcal{L}_{S_0}(U_\tau^i))$,

7: **return** $U_{\tau+1} = \psi(\Omega_{\tau+1})U_\tau \in \text{St}(r, \mathbb{R}^N)$

The choices of the coordinate map ψ and of the function $\mathcal{L}_{S_0} : \text{St}(r, \mathbb{C}^N) \rightarrow \mathfrak{u}(N)$ are clearly not unique. In this work, we aim at choosing them such that the arithmetic complexity of Algorithm 1 is at most linear in N excluding the computational cost associated with the evaluation of \mathcal{L}_{S_0} , which is problem dependent. To this aim it is crucial to deal with low-rank quantities in the application of both the coordinate map and its tangent inverse, as it will be shown in Proposition 4.2. Although the natural choice for \mathcal{L}_{S_0} would be $\mathcal{L}_{S_0}(U) = P(US_0U^*)$ for any $U \in \text{St}(r, \mathbb{C}^N)$, this quantity is typically not low-rank. We thus opt for the alternative, yet equivalent, choice $\mathcal{L}_{S_0}(U) = (I - UU^*)\mathcal{F}_{S_0}(U)U^* - U\mathcal{F}_{S_0}^*(U)$ where $\mathcal{F}_{S_0}(U) = P(US_0U^*)U$. Note that $\mathcal{L}_{S_0}(U) \in \mathfrak{u}(N)$ since $U^*\mathcal{F}_{S_0}(U) \in \mathfrak{u}(r)$ for any $U \in \text{St}(r, \mathbb{C}^N)$.

As coordinate map we consider the Cayley transform

$$\text{cay}(\Omega) := \left(I - \frac{\Omega}{2}\right)^{-1} \left(I + \frac{\Omega}{2}\right). \quad (4.4)$$

Proposition 4.2. *Let us consider the explicit RK-MK time integration scheme in Algorithm 1 for the approximation of problem (4.2) over the temporal interval \mathcal{I}_τ , $\tau \geq 0$. Let ψ be the Cayley transform (4.4). The arithmetic complexity of the algorithm is*

$$O(Nr^2N_s^2) + O(r^3N_s^4) + O(N^2rN_s) \quad (4.5)$$

where N_s is the number of stages of the underlying Runge–Kutta scheme.

Proof. The idea is that one can decompose $\mathcal{L}_{S_0}(U_\tau)$ into the sum of low-rank factors. Indeed, for any $i = 1, \dots, N_s$,

$$\mathcal{L}_{S_0}(U_\tau^i) = (I - U_\tau^i(U_\tau^i)^*)\mathcal{F}_{S_0}(U_\tau^i)(U_\tau^i)^* - U_\tau^i\mathcal{F}_{S_0}^*(U_\tau^i) = a_i b_i^* - U_\tau^i c_i^*$$

where $a_i := [\mathcal{F}_{S_0}(U_\tau^i) | -U_\tau^i] \in \mathbb{C}^{N \times 2r}$, $b_i := [U_\tau^i | \mathcal{F}_{S_0}(U_\tau^i)] \in \mathbb{C}^{N \times 2r}$, and $c_i := U_\tau^i \mathcal{F}_{S_0}^*(U_\tau^i) U_\tau^i \in \mathbb{C}^{N \times r}$. This implies that the inverse tangent map of the Cayley transform admits, in turn, a low-rank factorization:

$$\Lambda_i := d\psi_{\Omega_\tau^i}^{-1}(\mathcal{L}_{S_0}(U_\tau^i)) = d\psi_{\Omega_\tau^i}^{-1}(a_i b_i^* - U_\tau^i c_i^*) = A_\tau^i a_i (A_\tau^i b_i)^* - A_\tau^i U_\tau^i (A_\tau^i c_i)^* = \alpha_i \beta_i^*$$

where $\alpha_i := [A_\tau^i a_i | -A_\tau^i U_\tau^i] \in \mathbb{C}^{N \times 3r}$, $\beta_i := [A_\tau^i b_i | A_\tau^i c_i] \in \mathbb{C}^{N \times 3r}$ and $A_\tau^i := I - \Omega_\tau^i/2$.

The evaluation of $\mathcal{F}_{S_0}(U)$, for any $U \in \mathbb{C}^{N \times r}$, requires the computation of the stream matrix $P(US_0U^*)$ and its multiplication by U , for a total complexity of $O(N^2r)$. Then, given $\mathcal{L}_{S_0}(U_\tau^i)$, the computation of α_i and β_i requires $O(Nr \text{rank}(\Omega_\tau^i))$ operations. From the definition of Ω_τ^i at Line 3 of the algorithm and the properties of the matrices Λ_i , one has that $k_i := \text{rank}(\Omega_\tau^i) \leq 3r(i-1)$. This implies that the computation of U_τ^i at Line 4 requires $O(Nrk_i) + O(k_i^2r) + O(k_i^3)$, as shown in e.g. [29, Proposition 5.2]. The conclusion follows by summing these quantities. \square

Remark 4.2. *In this work we focus on the complexity reduction in the number of degrees of freedom N and consider numerical time integration schemes of order at most 2, i.e. with $N_s = 2$. For higher order timestepping, the polynomial complexity in the number N_s of stages in (4.5) can be mitigated by using tangent methods as the one proposed in [5].*

4.2 Properties of the approximate solution

Lemma 4.1. *Let $Y_\tau = U_\tau S_0 U_\tau^*$ be the approximate solution of problem (3.1) at time t_τ with U_τ obtained from a RK-MK method of order p as in Algorithm 1. Let $Y(t_\tau) = U(t_\tau) S_0 U^*(t_\tau)$ with $U(t_\tau)$ exact solution of (4.2) at time t_τ . Then, there exists a positive constant $c \in \mathbb{R}$ such that*

$$\|Y_\tau - Y(t_\tau)\| \leq c\Delta t^p \sqrt{\sum_{i=1}^r \sigma_i^2(W_0)}.$$

Proof. By simply applying triangle inequality, one gets

$$\|Y_\tau - Y(t_\tau)\| \leq \|U_\tau - U(t_\tau)\| \|S_0\| (\|U(t_\tau)\|_2 + \|U_\tau\|_2),$$

and $\|S_0\|^2 = \|Y_0\|^2 = \sum_{i=1}^r \sigma_i^2(W_0)$. \square

A bound on the approximation error $\|W(t_\tau) - Y_\tau\|$, for any τ , can be obtained by combining the above result with the bound (3.4) between the exact solution Y of (3.1) and the best low-rank approximation of W .

Lemma 4.2. *Let $Y_\tau = U_\tau S_0 U_\tau^*$ be the approximate solution of problem (3.1) at time t_τ with U_τ obtained from a RK-MK method as in Algorithm 1. The discrete flow of Y_τ is isospectral and the Casimir functions (2.5) satisfy, for any $1 \leq k \leq N$,*

$$|C_k(W(t_\tau)) - C_k(Y_\tau)| = \left| \sum_{j=r+1}^N \lambda_j^k(W_0) \right|.$$

Proof. Since the approximation U_τ of $U(t_\tau)$ obtained from Algorithm 1 belongs, by construction, to $\text{St}(r, \mathbb{C}^N)$ for any τ , the approximate solution $Y_\tau = U_\tau S_0 U_\tau^*$ belongs to $\mathbf{u}(N)$. As a consequence, the discrete flow of Y_τ is isospectral and the Casimir functions (2.5) are exactly preserved, that is, $|C_k(Y_\tau) - C_k(Y_0)| = 0$ for any τ and any $1 \leq k \leq N$. Combining this with (3.2) yields the result. \square

5 Approximation of the stream function

The computational cost of solving the discrete Laplace equation in (2.2) for the stream matrix P is the bottleneck of the algorithm, as shown in the proof of Proposition 4.2. One possibility to speed up its computation is to evaluate the stream function on an approximation of the vorticity matrix as follows. A very similar technique was introduced in [6] to filter large-scale components of the dynamics.

Let $0 < \widehat{N} \leq N - 1$, we introduce the operator $\mathcal{T}_{\widehat{N}} : \mathbb{C}^{N \times N} \rightarrow \mathbb{C}^{N \times N}$ that, when applied to W , sets to zero the j th diagonal of W for any $|j| > \widehat{N}$. When restricted to $\mathbf{u}(N)$, $\mathcal{T}_{\widehat{N}}$ can be written as

$$\mathcal{T}_{\widehat{N}} : W = \sum_{\ell=1}^{N-1} \sum_{m=-\ell}^{\ell} i\omega^{\ell m} T_{\ell,m}^N \mapsto \sum_{\ell=1}^{N-1} \sum_{m=-\min\{\ell, \widehat{N}\}}^{\min\{\ell, \widehat{N}\}} i\omega^{\ell m} T_{\ell,m}^N \quad (5.1)$$

Using this approximation in the solution of the Laplace equation in (2.2) yields the following evolution equation: given $Z(0) = Z_0 \in \mathbf{u}(N)$, find $Z \in C^1(0, T; \mathbf{u}(N))$ such that

$$\begin{cases} \dot{Z} = [\widehat{P}(Z), Z], \\ \Delta_N \widehat{P} = \mathcal{T}_{\widehat{N}}(Z), \end{cases} \quad (5.2)$$

where Δ_N is the Laplace operator from (2.3).

To show that the flow (5.2) is isospectral and Lie–Poisson we need the following technical, yet elementary, result.

Lemma 5.1. *Let the operator $\mathcal{T}_{\widehat{N}} : \mathbf{u}(N) \rightarrow \mathbf{u}(N)$ be defined as in (5.1) for some $0 < \widehat{N} \leq N - 1$. Then, $\mathcal{T}_{\widehat{N}}$ is linear, self-adjoint with respect to the Frobenius inner product and it commutes with Δ_N^{-1} , the inverse of the Laplace operator from (2.3).*

Owing to the properties of $\mathcal{T}_{\widehat{N}}$ from Lemma 5.1 and to the self-adjointness of Δ_N with respect to the Frobenius inner product, a result analogous to Lemma 2.1 holds for problem (5.2). In particular, the flow is isospectral and Hamiltonian but with respect to an approximate Hamiltonian, resulting from the approximation introduced by (5.1).

Lemma 5.2. *The dynamical system (5.2) is isospectral and Lie–Poisson on the dual of $\mathbf{u}(N)$ with Hamiltonian given by*

$$\widehat{H}(Z) = \frac{1}{2} \text{Tr}(\widehat{P}(Z)Z^*). \quad (5.3)$$

The error in the approximation of the Hamiltonian can be bounded by the error in the approximation of the initial condition and by the Hamiltonian approximation at the initial time, as follows. For any $t \in \mathcal{I}$, let $W(t)$ be the solution of (2.2) and let $Z(t)$ be solution of (5.2), then

$$|H(W(t)) - \widehat{H}(Z(t))| = |H(W_0) - \widehat{H}(Z_0)| \leq |H(W_0) - H(Z_0)| + |H(Z_0) - \widehat{H}(Z_0)|$$

Remark 5.1. *The approximation of the Laplace equation introduced in (5.2) can be applied also to the original problem (2.2). This is equivalent to solving problem (5.2) with initial condition $Z_0 = W_0$. In such situation the error in the approximation of the Hamiltonian is only due to the initial approximation error $|H(W_0) - \widehat{H}(W_0)|$.*

The approximation introduced by $\mathcal{T}_{\widehat{N}}$ has no effect on the Casimir invariants.

Concerning the accuracy of the approximation, we can establish an error bound analogous to Proposition 3.2 with a further term that depends on the truncation (5.1) and goes to zero as \widehat{N} tends to N .

Proposition 5.1. *For any $t \in (0, T]$, let $Z(t)$ be the solution of (5.2) with initial condition $Z_0 = Y_0$ and let $W^{\text{svd}}(t)$ be the best rank- r approximation of $W(t)$, where $W(t)$ is solution of (2.2). Then,*

$$\begin{aligned} \|Z(t) - W^{\text{svd}}(t)\| &\leq (1 + \widehat{K}^{-1}\gamma)(e^{\widehat{K}t} - 1) \sqrt{\sum_{i=r+1}^N \sigma_i^2(W_0)} \\ &\quad + \|W_0\| \int_0^t \|P(W(s)) - \widehat{P}(W(s))\| e^{\widehat{K}(t-s)} ds, \end{aligned} \quad (5.4)$$

where \widehat{K} is the Lipschitz continuity constant of $X_{\widehat{H}}$ and $\gamma := \|\Delta_N^{-1}\|_2 \|W_0\|$.

Proof. The reasoning is analogous to the proof of Proposition 3.2; here we need to consider the extra term associated with the approximation of H by \widehat{H} .

Using the evolution equations (3.3) for W^{svd} and (5.2) for Z gives

$$\begin{aligned} \|\dot{Z}(t) - \dot{W}^{\text{svd}}(t)\| &= \|X_{\widehat{H}}(Z) - [P(W), W^{\text{svd}}]\| \\ &\leq \|X_{\widehat{H}}(W) - X_{\widehat{H}}(Z)\| + \|X_H(W) - [P(W), W^{\text{svd}}]\| + \|X_H(W) - X_{\widehat{H}}(W)\|. \end{aligned} \quad (5.5)$$

The first two terms can be bounded as in the proof of Proposition 3.2 using the Lipschitz continuity of the Hamiltonian vector field $X_{\widehat{H}}$ and the linearity of the matrix commutator, resulting in

$$\|X_{\widehat{H}}(W) - X_{\widehat{H}}(Z)\| + \|X_H(W) - [P(W), W^{\text{svd}}]\| \leq \widehat{K}\|W - Z\| + \|\Delta_N^{-1}\|_2 \|W_0\| \|W - W^{\text{svd}}\|.$$

The last term in (5.5) can be bounded as

$$\|X_H(W) - X_{\widehat{H}}(W)\| = \|[P(W) - \widehat{P}(W), W]\| \leq \|P(W) - \widehat{P}(W)\| \|W_0\|.$$

Combining the bounds above we get, for any $t \geq 0$,

$$\|\dot{Z}(t) - \dot{W}^{\text{svd}}(t)\| \leq (\widehat{K} + \gamma)\|W(t) - W^{\text{svd}}(t)\| + \widehat{K}\|W^{\text{svd}}(t) - Z(t)\| + \|W_0\| \|P(W(t)) - \widehat{P}(W(t))\|$$

with $\gamma := \|\Delta_N^{-1}\|_2 \|W_0\|$. Using Gronwall's inequality and the fact that $\|W(t) - W^{\text{svd}}(t)\| = \|W_0 - W_0^{\text{svd}}\|$ yields the conclusion. \square

Note that the last term of (5.4) can be further bounded as

$$\|W_0\| \int_0^t \|P(W(s)) - \widehat{P}(W(s))\| e^{\widehat{K}(t-s)} ds \leq \gamma \int_0^t \|W(s) - \mathcal{T}_{\widehat{N}}(W(s))\| e^{\widehat{K}(t-s)} ds.$$

5.1 Computational complexity of the approximate dynamics

The approximation of the stream function introduced in (5.1) can be applied to both the original model (2.2) and to the approximate dynamics (3.1). In both cases the computational complexity is lowered by a factor N leading to a complexity quadratic in N for the original model and linear in N when solving the approximate model.

Proposition 5.2. *Let us consider the numerical time integration scheme (2.6)-(2.7) for the approximation of problem (5.2) over the temporal interval \mathcal{I}_τ , $\tau \geq 0$. The arithmetic complexity of the algorithm is*

$$O(N^2 \widehat{N} n_{\text{it}}^\tau)$$

where n_{it}^τ is the number of iterations required by the nonlinear step (2.6).

Proof. Repeating the steps of the proof of Proposition 2.1, one has that the stream matrix \widehat{P} satisfies an approximate Laplacian problem and it can be computed by solving $\widehat{N} + 1$ linear systems $\Delta^m p_m = z_m$ for $m = 0, \dots, \widehat{N}$, where p_m and z_m denote the m th diagonals of P and Z , respectively. Since each system has size $N - m$ and it is tridiagonal, the number of operations required is $\sum_{m=0}^{\widehat{N}} (N - m)$, thus leading arithmetic complexity $O(N\widehat{N})$.

Moreover, at the j th iteration of the nonlinear solver (2.6), the computation of the bracket two matrix-matrix multiplications involving the sparse stream matrix. These yields $O(N^2 \widehat{N})$ operations for each update of $\widetilde{W}^{(j)}$ and W_τ , namely $n_{\text{it}}^\tau + 1$ times. \square

The approximation of the stream function (5.1) in the approximate model (3.1) can be combined to the factorization of the state proposed in Section 4 leading to the evolution equation: given $U(t_0) = U_0 \in \text{St}(r, \mathbb{C}^N)$, find $U(t) \in \text{St}(r, \mathbb{C}^N)$ such that

$$\begin{cases} \dot{U} = \widehat{P}(US_0U^*)U, \\ \Delta_N \widehat{P} = \mathcal{T}_{\widehat{N}}(US_0U^*). \end{cases} \quad (5.6)$$

Proposition 5.3. *Let us consider the explicit RK-MK time integration scheme in Algorithm 1 for the approximation of problem (5.6) over the temporal interval I_{cal_τ} , $\tau \geq 0$. Let ψ be the Cayley transform (4.4). The arithmetic complexity of the algorithm is*

$$O(Nr^2N_s^2) + O(r^3N_s^4) + O(N\widehat{N}rN_s)$$

where N_s is the number of stages of the underlying Runge-Kutta scheme.

Proof. The reasoning is analogous to the proof of Proposition 4.2. The only part that changes is the cost to evaluate the term $\widehat{\mathcal{F}}(U) := \widehat{P}(US_0U)U$ for any $U \in \mathbb{C}^{N \times r}$.

To solve the approximate stream matrix one needs to reconstruct the m th diagonals of the state $Y := US_0U$ only for $0 \leq m \leq \widehat{N}$. The arithmetic of computing the m th diagonal of Y is $O(r(N-m))$. The total cost to assemble the right hand side of the approximate Laplace equation is thus $r \sum_{m=0}^{\widehat{N}} (N-m)$, i.e., $O(N\widehat{N}r)$. The solution of the approximate Laplace equation is then $O(N\widehat{N})$ and the matrix-matrix multiplication costs $O(Nr)$ owing to the sparsity of \widehat{P} .

The result follows by combining this cost with the arithmetic complexities derived in the proof of Proposition 4.2 for the intermediate steps of the RK-MK time integrator. \square

6 Approximate dynamics via splitting

Another possibility to perform a low-rank approximation of problem (2.2) is to consider the factorization of the approximate state, at any time $t \in \mathcal{I}$, given by

$$Y(t) = U(t)S(t)U^*(t) \quad \text{in } \mathcal{M}_r. \quad (6.1)$$

At the initial time we set $U(t_0) = U_0 \in \mathbb{C}^{N \times r}$ where the columns of U_0 are the eigenvectors associated with the r largest eigenvalues of W_0 , initial condition of the original problem (2.2), and $S_0 \in \mathbb{C}^{r \times r}$ contains the r largest eigenvalues of W_0 . Moreover, we require that, for any $t \in \mathcal{I}$, $U(t)$ belongs to the Stiefel manifold $\text{St}(r, \mathbb{C}^N)$ and $S(t) \in \mathbb{C}^{r \times r}$ is skew-Hermitian. These two conditions ensures that $Y(t) \in \mathfrak{u}(N)$ for any $t \in \mathcal{I}$. Moreover, if U is unitary, then $\text{Tr}(Y^k) = \text{Tr}(S^k)$ for any $k \geq 1$. Note that, differently from the factorization (4.1), we allow both U and S to vary in time. The factorization (6.1) is less preferable than (4.1) when dealing with isospectral flows but it is suitable for more general flows on $\mathfrak{u}(N)$ and it can be easily adapted to other matrix algebras.

To derive evolution equations for the factors U and S in (6.1), we propose the following decomposition of the velocity field

$$X_H(Y) = \underbrace{\Pi_{\mathcal{R}(U)} X_H(Y) \Pi_{\mathcal{R}^\perp(U)} + \Pi_{\mathcal{R}^\perp(U)} X_H(Y) \Pi_{\mathcal{R}(U)}}_{=: \Pi_U(X_H(Y))} + \underbrace{\Pi_{\mathcal{R}(U)} X_H(Y) \Pi_{\mathcal{R}(U)}}_{=: \Pi_S(X_H(Y))}, \quad (6.2)$$

where $\Pi_{\mathcal{R}(U)}$ is the orthogonal projections onto the range of U . Note that such decomposition holds for the orthogonal, with respect to the Frobenius norm, projection onto $T_Y \mathcal{M}_r$ of any vector field, that is $\Pi_{T_Y \mathcal{M}_r} X = \Pi_U(X) + \Pi_S(X)$ for any $X \in \mathbb{C}^{N \times N}$ and $Y \in \mathcal{M}_r$. Exploiting the decomposition of X_H introduced above we can split the evolution equation for Y in (3.1) into the following evolution equations:

$$\begin{cases} \dot{S} = U^* X_H(USU^*) U = [U^* P(USU^*) U, S], \\ \dot{U} = (I - UU^*) P(USU^*) U. \end{cases} \quad (6.3)$$

$$(6.4)$$

This system retains the geometric properties of the approximate model (3.1).

Proposition 6.1. *Let $U \in \text{St}(r, \mathbb{C}^N)$ be fixed, then problem (6.3) with $U(t) = U$, for any $t \in \mathcal{I}$, is isospectral and Lie-Poisson on the dual of $\mathfrak{u}(r)$ with Hamiltonian given by*

$$H_U(S) := H(USU^*) = \frac{1}{2} \text{Tr}(P(USU^*)US^*U^*).$$

Moreover, the evolution of U in (6.4) remains on the Stiefel manifold and the Hamiltonian is a conserved quantity whenever S is fixed, as shown in the following result.

Proposition 6.2. *Let $U(t)$ be solution of (6.4) with initial condition $U_0 \in \text{St}(r, \mathbb{C}^N)$. Then, $U(t)$ belongs to $\text{St}(r, \mathbb{C}^N)$ for any $t \in \mathcal{I}$. Moreover, if $Y = USU^*$ with $\mathbb{S} \in \mathfrak{u}(r)$ fixed, the Hamiltonian $H(Y)$ defined in (2.4) is conserved.*

Proof. To show that the trajectory of (6.4) remains on the Stiefel manifold $\text{St}(r, \mathbb{C}^N)$ one can simply verify that $d_t(U^*(t)U(t)) = 0$ for all t . Since $U_0 \in \text{St}(r, \mathbb{C}^N)$ by assumption, the conclusion follows.

To show the conservation of the Hamiltonian, we first write the evolution equation for $Y = USU^*$ based on (6.4); thereby

$$\dot{Y} = \dot{U}SU^* + US\dot{U}^* = [P(Y), Y] - U[U^*P(Y)U, \mathbb{S}]U^*.$$

Using this expression for \dot{Y} and the self-adjointness of the inverse Laplace operator yields

$$\begin{aligned} \frac{d}{dt}H(Y) &= \frac{1}{2} \langle P(\dot{Y}), Y \rangle + \frac{1}{2} \langle P(Y), \dot{Y} \rangle = \frac{1}{2} \langle \Delta_N^{-1}(\dot{Y}), Y \rangle + \frac{1}{2} \langle P(Y), \dot{Y} \rangle \\ &= \langle P(Y), [P(Y), Y] \rangle + \langle P(Y), U[U^*P(Y)U, \mathbb{S}]U^* \rangle \\ &= \langle U^*P(Y)U, [U^*P(Y)U, \mathbb{S}] \rangle = 0. \end{aligned}$$

□

Note that results analogous to Propositions 6.1 and 6.2 hold if we introduce in (6.3)-(6.4) the approximation of the stream function P from Section 5 with the Hamiltonian given by $\widehat{H}_r(S) = \frac{1}{2} \text{Tr}(\widehat{P}(USU^*)US^*U^*)$.

Corollary 6.1. *Let $t \in \mathcal{I}$ be fixed. Assume $Y(t) = U(t)S(t)U^*(t)$ is obtained from $S(t)$ solution of (6.3) and $U(t)$ solution of (6.4). Then $Y(t)$ belongs to $\mathcal{M}_r \cap \mathfrak{u}(N)$. Moreover, the Casimir functions (2.5) satisfy $C_k(Y(t)) = C_k(S(t))$, for any $k \geq 1$, and are, thus, conserved quantities.*

6.1 Time integration of the approximate dynamics via splitting

Let Φ_U and Φ_S denote the flux associated with the projection operator Π_U and Π_S from (6.2), respectively, so that $\Phi_U(t_\tau, t_{\tau+1}, Y(t_\tau))$ is solution of $\dot{Y} = \Pi_U(\dot{Y})$ in $\mathcal{I}_\tau = (t_\tau, t_{\tau+1}]$, with $\tau \geq 0$ and similarly for Φ_S . Problem (6.3)-(6.4) can be solved using a splitting scheme. We focus on a second order consistent splitting, such as the Strang splitting, since the lowest order isospectral Lie–Poisson integrator of [24] has order 2.

The Strang splitting integrator in the time interval \mathcal{I}_τ reads

$$Y_{\tau+1} = \Phi_U\left(t_{\tau+1/2}, t_{\tau+1}, \Phi_S\left(t_\tau, t_{\tau+1}, \Phi_U\left(t_\tau, t_{\tau+1/2}, Y_\tau\right)\right)\right).$$

Given $Y(t_\tau) = U(t_\tau)S(t_\tau)U^*(t_\tau)$, perform the following steps in \mathcal{I}_τ .

- Starting from the initial condition $U(t_\tau)$, derive $U(t_{\tau+1/2})$ by solving the $N \times r$ problem

$$\dot{U}(t) = (I - U(t)U^*(t))P(U(t)\mathbb{S}U^*(t))U(t) \quad \text{for } t \in (t_\tau, t_{\tau+1/2}], \quad (6.5)$$

with $\mathbb{S} = S(t_\tau)$.

- Starting from the initial condition $S(t_\tau)$, derive $S(t_{\tau+1})$ by solving the $r \times r$ problem

$$\dot{S}(t) = [\mathbb{U}^*P(\mathbb{U}S(t)\mathbb{U}^*)\mathbb{U}, S(t)] \quad \text{for } t \in (t_\tau, t_{\tau+1}], \quad (6.6)$$

with $\mathbb{U} = U(t_{\tau+1/2})$.

- Starting from the initial condition $U(t_{\tau+1/2})$, derive $U(t_{\tau+1})$ by solving problem (6.5) in $(t_{\tau+1/2}, t_{\tau+1}]$, with $\mathbb{S} = S(t_{\tau+1})$.

Then, return $Y(t_{\tau+1}) = U(t_{\tau+1})S(t_{\tau+1})U^*(t_{\tau+1})$.

The Hamiltonian is conserved by the splitting owing to Propositions 6.1 and 6.2. Taking $\mathbb{U} = U(t_{\tau+1/2})$, $\mathbb{S}_\tau = S(t_\tau)$, and $\mathbb{S}_{\tau+1} = S(t_{\tau+1})$ results in

$$\begin{aligned} H(Y(t_{\tau+1})) &= H(U(t_{\tau+1/2})\mathbb{S}_{\tau+1}U^*(t_{\tau+1/2})) = H_{\mathbb{U}}(S(t_{\tau+1})) = H_{\mathbb{U}}(S(t_\tau)) \\ &= H(U(t_{\tau+1/2})\mathbb{S}_\tau U^*(t_{\tau+1/2})) = H(U(t_\tau)\mathbb{S}_\tau U^*(t_\tau)) = H(Y(t_\tau)). \end{aligned}$$

Similarly, the Casimir functions are preserved since the factor S satisfies an isospectral flow and the factor U is unitary.

Remark 6.1. *In principle one could solve problem (6.3)-(6.4) via the DLRA splitting integrator introduced in [22] or one of its extensions. However, the conservation of the Casimirs is not guaranteed: for one, integrating the evolution equation (6.3) for S from the initial condition $S(t_\tau) = (U^*(t_{\tau+1})U(t_\tau))S(t_\tau)(U^*(t_{\tau+1})U(t_\tau))^*$ prevents the flow of S from being isospectral. Moreover, the Hamiltonian is, in general, no longer globally conserved.*

The evolution equation for the low-dimensional factor S in (6.3) can be solved using the isospectral and Lie–Poisson integrator proposed in [24]. The time integrator is as in (2.6)-(2.7) with the stream function P replaced by U^*PU . The evolution equation for the factor U can be solved using a RK-MK time integrator as described in Section 4.1.

By construction these numerical time integrators combined with the splitting ensure that $S_\tau \in \mathfrak{u}(r)$ and $U_\tau \in \text{St}(r, \mathbb{C}^N)$ for any $\tau \geq 0$, which gives $Y_\tau = U_\tau S_\tau U_\tau^* \in \mathfrak{u}(N)$ for any $\tau \geq 0$. Moreover, the Casimir functions are preserved by the temporal discretization.

6.2 Computational complexity of solving the approximate dynamics

The computational complexity of solving the evolution equation for S , in the temporal subinterval \mathcal{I}_τ , with the isospectral scheme of Section 2.2 is $O(N^2 r n_{\text{it}}^\tau) + O(r^3 n_{\text{it}}^\tau)$ where n_{it}^τ is the number of iterations required by the nonlinear step (2.6). This can be easily verified by reproducing the steps of the proof of Proposition 2.1. The evolution of the factor U in (6.4) solved with a RK-MK time integrator has the arithmetic complexity proven in Proposition 4.2, namely $O(Nr^2 N_s^2) + O(r^3 N_s^4) + O(N^2 r N_s)$. The proof goes as the one of Proposition 4.2 with $\mathcal{L}_S(U) := \mathcal{F}_S(U)U^* - U\mathcal{F}_S^*(U)$ and $\mathcal{F}_S(U) = (I - UU^*)P(USU^*)U$. This means that, contrary to the solver for the original model, see Proposition 2.1, the proposed low-rank splitting scales quadratically with N .

When the stream function P is approximated as in Section 5, then the computational complexity of the algorithm in the time interval \mathcal{I}_τ reduces to

$$O(N\hat{N}r^2 n_{\text{it}}^\tau) + O(r^3 n_{\text{it}}^\tau) + O(Nr^2 N_s^2) + O(r^3 N_s^4) + O(N\hat{N}r N_s).$$

7 Numerical experiments

We test the performances of the proposed methods on two test cases. In the first one we consider as initial condition a random skew-Hermitian matrix with a prescribed spectrum. In the second test case we consider a more physical simulation of point-vortex dynamics.

Concerning the notation, if not otherwise specified, the symbol W_{ref} will denote a reference solution, W^{svd} the truncated SVD of W_{ref} , and Ω a generic numerical solution. In the legend we will use the shorthand “Om” to refer to the original model (2.2), “Am(r)” to refer to the approximate model (3.1) with rank r , and “TAm(r, \hat{N})” to refer to the approximate model with truncation (5.2) with rank r and truncation to the \hat{N} th mode.

We compare different time integrators: Iso-2 refers to the second order isospectral Lie–Poisson integrator of [24] and summarized in Section 2.2; RKMK-p, with $p \in \{1, 2\}$, refers to the p th order Runge–Kutta Munthe-Kaas time integrator described in Section 4.1 for the solution of the evolution equation (4.2) (or (6.5)) for the factor U in the low-rank factorization (4.1) (or (6.1)).

7.1 Random initial condition with prescribed spectrum

Given N , we consider as initial condition a matrix $W_0 \in \mathfrak{u}(N)$ generated randomly from a standard normal distribution but with prescribed spectrum as given in Figure 1 (for the case $N = 500$). We assess the performances of the different algorithms by comparison with a reference solution W_{ref} obtained by solving the original model (2.2) with initial condition W_0 , N degrees of freedom, and the second order isospectral solver Iso-2 with a fine time step Δt that will be specified case by case. We compare the different algorithms on the temporal interval $[0, T = 1]$.

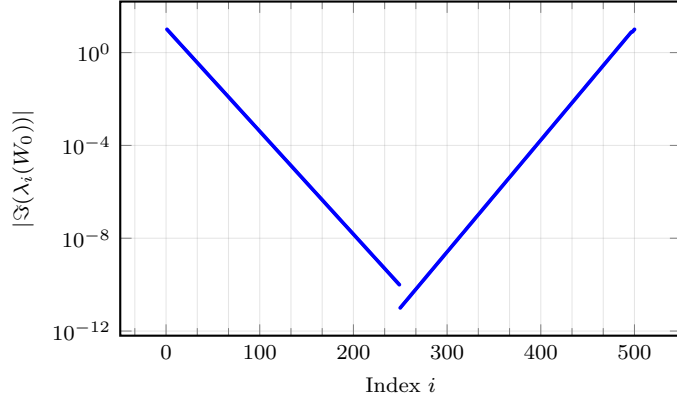


Figure 1: Absolute value of the imaginary part of the eigenvalues of the initial state W_0 for $N = 500$.

7.1.1 Full-rank approximation $r = N$, different time steps Δt

As a first test we set $N = 100$ and compute the reference solution W_{ref} using `Iso-2` with $\Delta t = 10^{-6}$. We take the approximation rank r equal to the problem dimension N and let Δt vary. This allows us to assess the performances of the numerical time integration schemes and of the factorization (4.1) without considering the error introduced by a low-rank approximation. In Figure 2 we show the error in the Frobenius norm between the reference solution $W_{\text{ref}}(T)$ at final time $T = 1$ and an approximation $\Omega(T)$. We compare the cases where Ω is obtained by solving the original model (2.2) with the `Iso-2` scheme and the full-rank approximate model (3.1)-(4.2) with the RK-MK time integrator of order one and two. In Figure 2 we observe that, as expected, all numerical solutions converge to the reference one with the order of the corresponding scheme. We also record that, at least in this test case, the error obtained with the approximate model (red line with stars) is lower than the one obtained with the original model and `Iso-2` solver (blue line with dots).

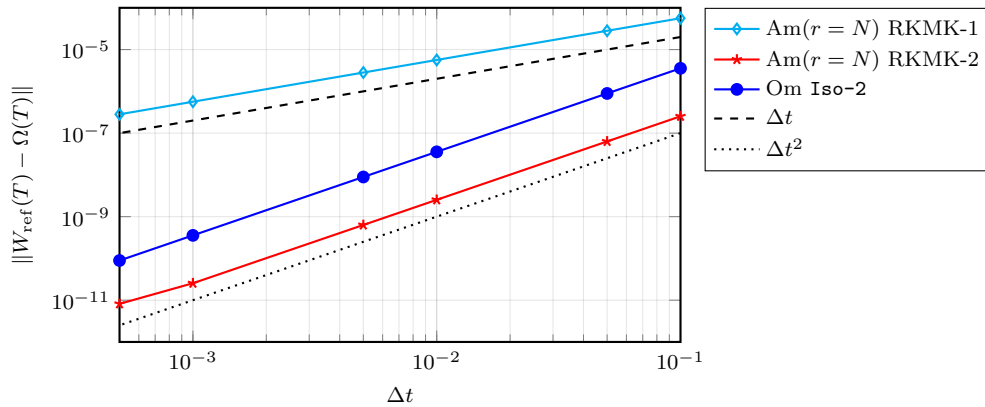


Figure 2: Error, at the final time T , between the reference solution and different approximate solutions vs. the time step Δt .

We also study the runtime of each algorithm taking into account the accuracy of the approximation. In Figure 3 we report the error between the reference and the approximate solutions versus the algorithm runtime (in seconds). Each datum refers to a different value of Δt with $\Delta t \in \{5e-4, 1e-3, 5e-3, 1e-2, 5e-2, 1e-1\}$. We observe that the second order RK-MK solver used to solve the approximate model (red line with stars) is computationally more efficient than solving the original with `Iso-2` (blue line with dots), for a given time step Δt . As an example an error of the order of 10^{-9} is achieved with the second order approximate solver 8 times faster than with the original model.

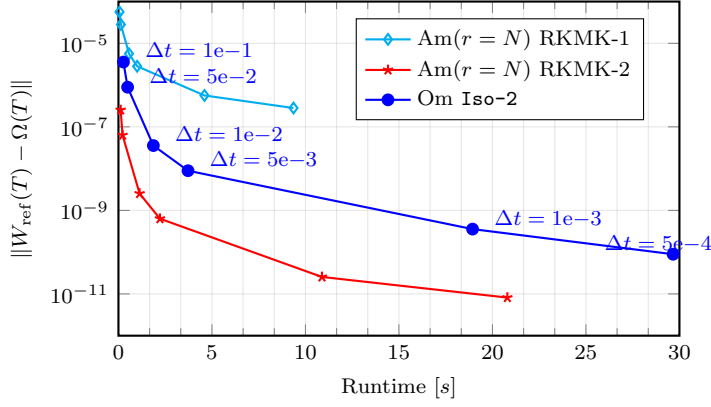


Figure 3: Error between the reference solution and different approximate solutions vs. algorithm runtime. Each datum refers to a different value of Δt .

7.1.2 Fixed time step Δt , different approximation ranks r

In this test case we fix $N = 500$ and compute the reference solution W_{ref} using the second order isospectral integrator `Iso-2` with $\Delta t = 10^{-5}$. We want to compare the approximate solution also with the best low-rank approximation W^{svd} given by the truncated SVD of W_{ref} at each time.

As time integrator for the evolution equation (4.2) of the factor U in (4.1) we consider the second order RK-MK scheme with $\Delta t = 10^{-2}$.

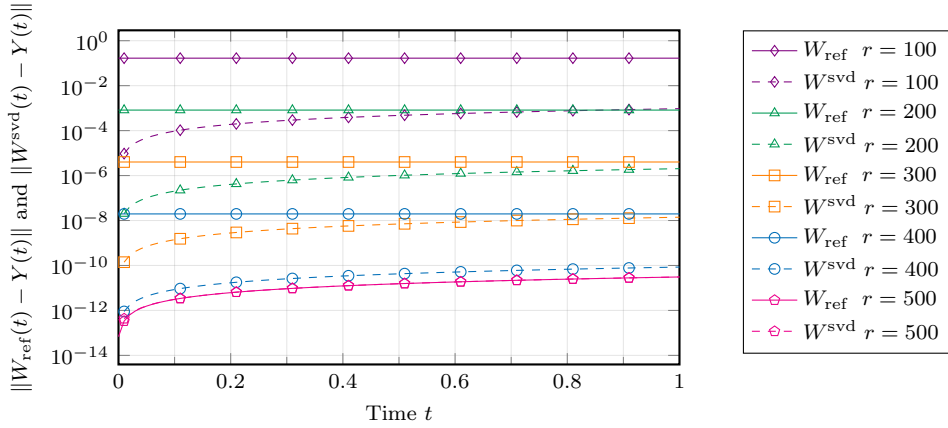


Figure 4: Evolution of the error between the approximate solution and the reference solution (solid lines) and of the error between the approximate solution and the best low-rank approximation (dashed lines). The different lines refer to different ranks r .

In Figure 4 we report the evolution of the error $\|Y(t) - W_{\text{ref}}(t)\|$ between the reduced order solution and the reference solution and of the error $\|Y(t) - W^{\text{svd}}(t)\|$ between the reduced order solution and the best low-rank approximation of the reference solution. Each line is associated to a fixed rank r with $r \in \{100, 200, 300, 400, 500\}$. We observe that the error with respect to the reference solution has small variation in time. Moreover, we can infer that the distance between the approximate trajectory and the best low-rank approximation is lower than the approximation error due to the low-rank truncation. This is further confirmed in Figure 5 where the different errors at final time are plotted against the rank r .

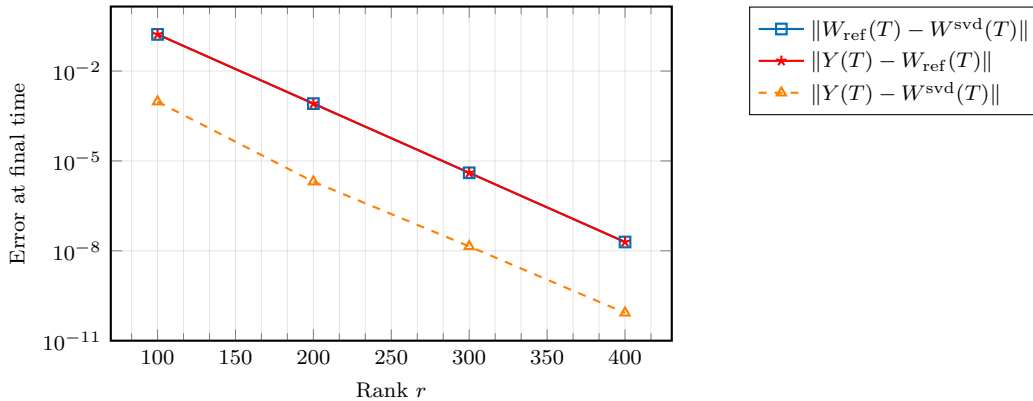


Figure 5: Approximation errors at the final time vs. the approximation rank r .

To assess the performances of the low-rank approximation in terms of computational efficiency, we report in Figure 6 the error between the reference solution and the approximate solution versus the algorithm runtime. The blue line with dots refers to the solution of the original model (2.2) using the Iso-2 scheme, while the red line with crosses refers to the low-rank approximation (4.1). We observe that, although the computational cost of solving the low-rank model increases with its size r , as expected, it is always lower than the cost required to solve the original model. In particular, from the left plot we can infer that the approximate model can achieve a more accurate solution at a lower computational cost, see for example the case $r = N = 500$.

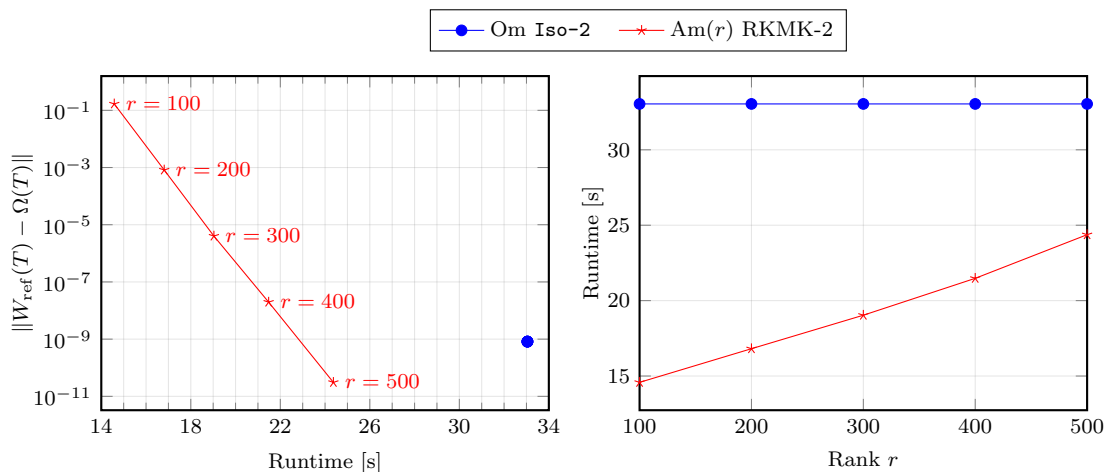


Figure 6: Left: error between the reference solution and the solution of the original model and error between the reference solution and the approximate low-rank solution versus the algorithm runtime. Right: algorithm runtime vs. the approximation rank r .

Figure 7 shows the error in the Hamiltonian evaluated at the low-rank approximate solution is only due to the quality of the low-rank approximation at the initial time (left plot) and it decreases as r grows, as expected. The Hamiltonian is preserved by the low-rank approximate trajectories to machine precision and independently of r (not shown here).

To check the numerical conservation of the Casimir invariants we look at the error in the eigenvalues of the approximate solution. In Figure 7 we report the ℓ^∞ error between the eigenvalues of the solution at final time and of the initial reference solution. Note that the error is constant in time since both temporal integrators are isospectral and it only depends on the neglected eigenvalues associated with the low-rank factorization. As expected, the solution obtained with the Iso-2 solver preserves the eigenvalues and, hence, the Casimirs to machine precision (blue lines with dots). Concerning the low-rank approximation, the error in the eigenvalues decreases as the rank r increases.

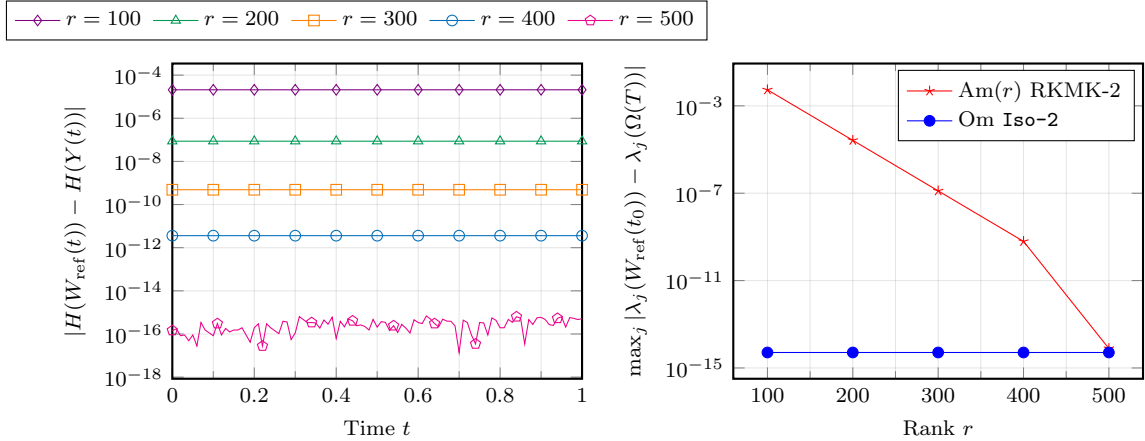


Figure 7: Left: evolution of the error between the Hamiltonian evaluated at the reference solution and the Hamiltonian evaluated at the low-rank approximate solution. Different ranks r are considered. Right: Error between the eigenvalues of the low-rank approximate solution at final time and the eigenvalues of the reference solution at initial time vs. the rank r of the approximation.

7.2 Point-vortex dynamics

Point-vortex dynamics describes the evolution of solutions where the vorticity is characterized by a finite sum of Dirac distributions. Point vortices are used to study geophysical turbulence.

In this test we consider four point vortices distributed, at the initial time, according to

$$R_j = \exp(100\sqrt{N}(ia_j(T_{1,1}^N - T_{1,-1}^N) - b_j(T_{1,1}^N + T_{1,-1}^N) + ic_j T_{1,0}^N)), \quad j \in \{1, 2, 3, 4\}$$

where a_j, b_j, c_j are random real numbers and the matrices $T_{\ell,m}^N$ are defined according to (2.3). The initial condition is then

$$W_0 = 2i \sum_{j=1}^4 R_j^\top B R_j$$

where $B \in \mathbb{C}^{N \times N}$ has zero entries except for $B_{N,N} = 1$.

We set $N = 500$. The reference solution is obtained by solving the original model (2.2) with the isospectral Lie-Poisson solver `Iso-2` of [24] with $\Delta t = 0.1$. The reference solution at the initial and final times is reported in Figure 8. The numerical final time is $T = 63000$.

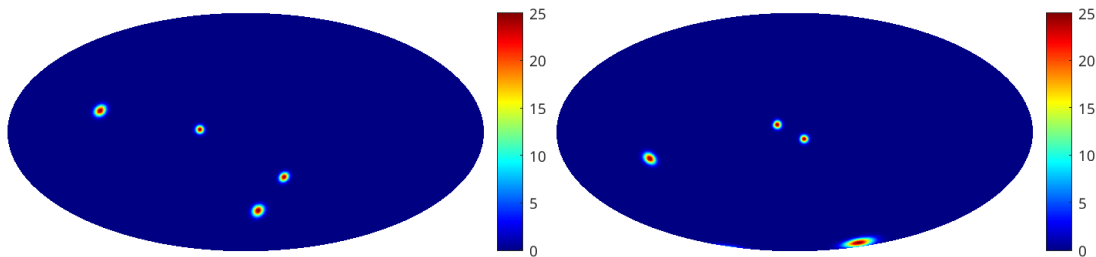


Figure 8: Reference solution at the initial time (left) and at the final time (right).

In this test we compare the performances of the original model (2.2) solved with `Iso-2` and the low-rank approximate models with rank $r = 4$ which corresponds to the actual rank of the vorticity matrix for this test case. In tests that, for the sake of brevity, we do not report here we observe that there is no improvement in performing a low-rank approximation with rank $r > 4$, as expected. In such situations the accuracy does not improve but the computational cost is higher than in the case $r = 4$. Taking $r < 4$, we observe, at every time, an error proportional to the best rank- r approximation error at the initial time and, thus, proportional to the magnitude of the neglected singular values of W_0 . In view of these results we focus on the case $r = 4$.

In Figure 9 we compare the performances of the original model and of the low-rank approximation in terms of accuracy and computational cost. We let the time step Δt vary and compute the errors

with respect to the reference solution at the final time T . We observe that, for a fixed Δt , the low-rank approximation yields a smaller error at a lower computational cost.

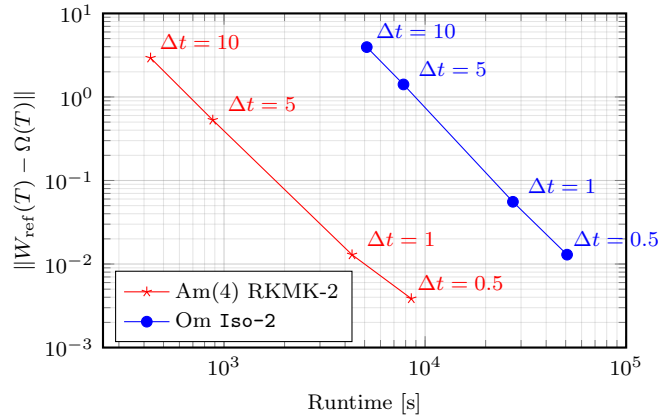


Figure 9: Error, at the final time, between the reference solution and the solution of the approximate low-rank model (3.1) and error between the reference solution and the solution of the original model (2.2) versus the algorithm runtime. Different values of the time step Δt are considered.

In a second set of numerical experiments we fix $r = 4$ and the time step $\Delta t = 1$ and study the performances of the low-rank approximation with and without truncation of the stream matrix, see Section 5. Figure 10 reports the error at the final time vs. the algorithm runtime of the low-rank approximation with and without the truncation. It can be observed that the low-rank model with truncation is computationally cheaper than solving the low-rank model without truncation but at the cost of a decrease in accuracy when $\hat{N} < 75$. For a truncation size \hat{N} equal to 75 or larger the low-rank approximation with truncation achieves the error of the low-rank approximation, and, for $\hat{N} = 75$, at less than half of the computational cost. The original model requires 27334 s to achieve an error of $5.55e-2$, and it is not reported in the figure. This means that it is roughly 17 times more expensive than the truncated low-rank model with $\hat{N} = 75$ and has even a slightly larger error.

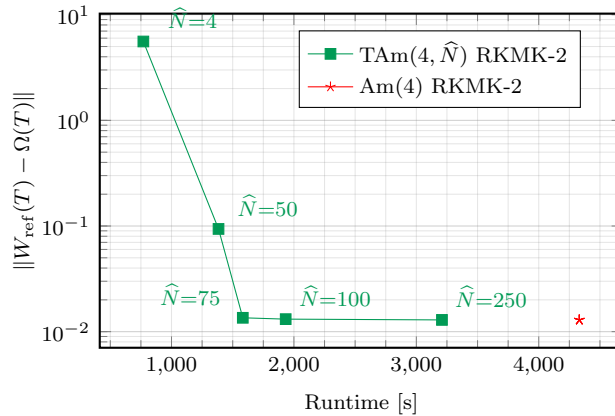


Figure 10: Error of the solution of the approximate low-rank model (3.1) and error of the solution of the approximate low-rank model with truncation (5.2) versus the algorithm runtime, for different values of the truncation size \hat{N} .

In Figure 11 (left plot) we report the error in the conservation of the Hamiltonian. Exact conservation of the Hamiltonian is not expected from the proposed numerical time integration schemes. We observe that the reference solution has a smaller error than the other trajectories and this is associated with the smaller time step used. The low-rank approximations have a similar behavior to the solution of the original model in terms of Hamiltonian conservation, with a slightly lower error. On the right plot of Figure 11, it is reported the evolution of the error between the Hamiltonian evaluated at the reference solution and at the low-rank approximation with truncation. Different truncation sizes \hat{N} are considered. As predicted by the theory, the truncated model is Hamiltonian

with a Hamiltonian \widehat{H} (5.3) that is an approximation of the original one. As \widehat{N} increases the error in the approximation of the Hamiltonian decreases, and for $\widehat{N} > 75$ the truncation is no longer affecting the accuracy of the approximation.

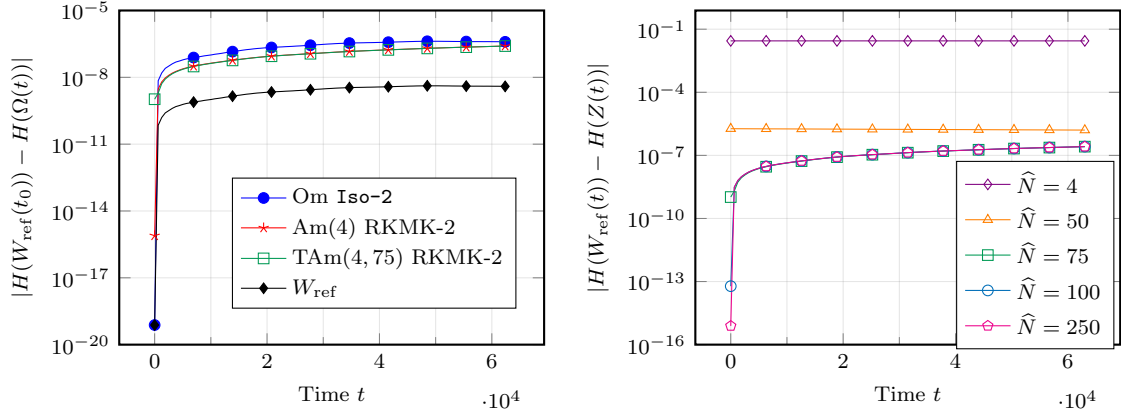


Figure 11: Left: Conservation of the Hamiltonian. Right: evolution of the error between the Hamiltonian evaluated at the reference solution and the Hamiltonian evaluated at the low-rank approximate solution of (5.2) for different values of the truncation size \widehat{N} .

The conservation of the Casimir functions is numerically studied in Figure 12, where we plot the evolution of the ℓ^∞ error between the eigenvalues of the solution at each time and of the initial reference solution. While some numerical errors are affecting the solution of the original model, the low-rank approximations preserve the 4 dominant eigenvalues to almost machine precision.

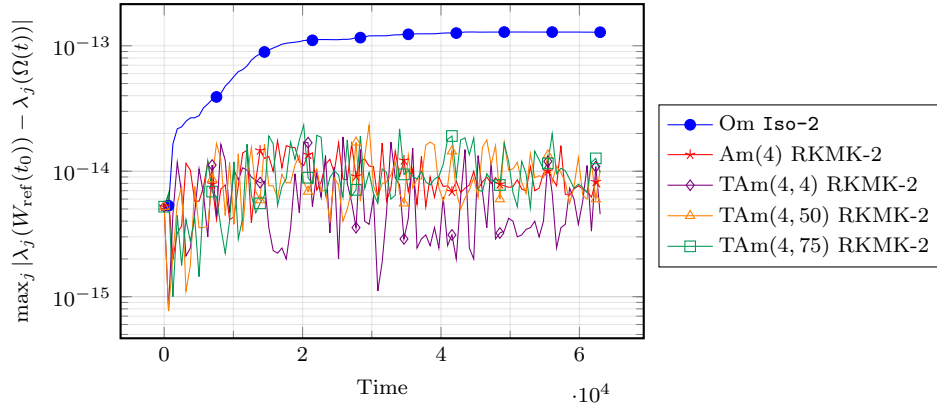


Figure 12: Error between the eigenvalues of the low-rank approximate solution at final time and the eigenvalues of the reference solution at initial time vs. the rank r of the approximation.

In Figure 13 we report the solution at the final time obtained with the: original model solved with **Iso-2** (left); low-rank approximate model with $r = 4$ (center); and low-rank approximate model with $r = 4$ and a truncation to $\widehat{N} = 75$ (right). Comparing with the reference solution in Figure 8, we observe that all models and numerical methods are able to reproduce a qualitatively correct behavior of the solution.

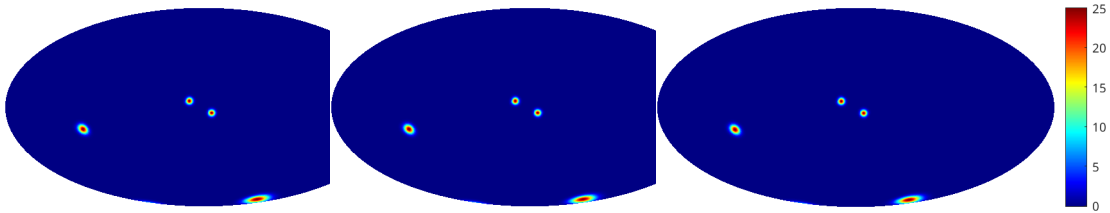


Figure 13: Approximate solutions at final time: original model solved with **Iso-2** (left), low-rank approximate model with $r = 4$ (center), low-rank approximate model with $r = 4$ and a truncation to $\widehat{N} = 75$ (right).

As a final test, we consider the low-rank approximation with the factorization proposed in Section 6, namely where the factor S is time-dependent. The problem parameters are as described above. In the temporal splitting of Section 6, the evolution equation for U in (6.5) is solved using a RK-MK integrator of order 2, while the evolution of S in (6.6) is solved with Iso-2. In Table 1 we compare the performances of the original model, low-rank approximation (4.1) with fixed factor S_0 , and the low-rank approximation (6.1) with time-dependent S . We observe that the low-rank approximation with splitting is slightly more accurate than the other models, both in the solution and in the Hamiltonian conservation. Compared to the factorization with S_0 fixed, the model with time-dependent S is considerably computationally more expensive (by almost 4.5 times), although it is cheaper than solving the original model (2.2). This suggests that the factorization (6.1) together with the temporal splitting of Section 6 is a valid low-rank approximation and it is best suited for flows on matrix manifolds that are not isospectral.

Table 1: Comparison of the original model (2.2), the low-rank approximation with factorization (4.1) and the low-rank approximation (6.1) with time-dependent S .

	Om with Iso-2	Am(4) with S_0	Am(4) with $S(t)$
$\ W_{\text{ref}}(T) - \Omega(T)\ $	5.55e-2	1.29e-2	5.30e-3
$\max_{\tau} \ H(W_{\text{ref}}(t_0)) - H(\Omega(t_{\tau}))\ $	4.15e-7	2.57e-7	3.21e-8
Runtime [s]	27334	4331	19322

8 Concluding remarks

We have proposed a low-rank approximation of the Zeitlin model that provides a finite-dimensional description of the incompressible Euler equations on the sphere. Two factorizations of the vorticity matrix have been considered: one based on a eigendecomposition where only the basis of eigenvectors depends on time, and a second one where all factors are time-dependent. Despite having both structure-preserving and favorable approximability properties, the first turns out to be more suitable for isospectral flow, while the second factorization might be used for other type of Euler–Arnold equations. Extensive numerical experiments on the latter are left for future work.

Acknowledgments

The author would like to thank Klas Modin for inspiring discussions on various aspects of the Zeitlin model. Several discussions with Arnout Franken and Erwin Luesink in a preliminary stage of this work, and with Milo Viviani are also gratefully acknowledged.

References

- [1] V. I. Arnold. “Sur la géométrie différentielle des groupes de Lie de dimension infinie et ses applications à l’hydrodynamique des fluides parfaits”. fr. *Annales de l’Institut Fourier* 16.1 (1966), pp. 319–361.
- [2] V. I. Arnold and B. A. Khesin. *Topological methods in hydrodynamics*. Vol. 125. Applied Mathematical Sciences. Springer-Verlag, New York, 1998.
- [3] M. Bordemann, J. Hoppe, P. Schaller, and M. Schlichenmaier. “ $\text{gl}(\infty)$ and geometric quantization”. *Comm. Math. Phys.* 138.2 (1991), pp. 209–244.
- [4] M. Bordemann, E. Meinrenken, and M. Schlichenmaier. “Toeplitz quantization of Kähler manifolds and $\text{gl}(N)$, $N \rightarrow \infty$ limits”. *Comm. Math. Phys.* 165.2 (1994), pp. 281–296.
- [5] E. Celledoni and B. Owren. “A class of intrinsic schemes for orthogonal integration”. *SIAM J. Numer. Anal.* 40.6 (2002), pp. 2069–2084.
- [6] P. Cifani, S. Ephrati, and M. Viviani. “Sparse-Stochastic Model Reduction for 2D Euler Equations”. *Stochastic Transport in Upper Ocean Dynamics II*. Ed. by B. Chapron, D. Crisan, D. Holm, E. Mémin, and A. Radomska. Cham: Springer Nature Switzerland, 2024, pp. 17–28.

- [7] P. Cifani, M. Viviani, E. Luesink, K. Modin, and B. J. Geurts. “Casimir preserving spectrum of two-dimensional turbulence”. *Phys. Rev. Fluids* 7 (8 2022), p. L082601.
- [8] P. Cifani, M. Viviani, and K. Modin. “An efficient geometric method for incompressible hydrodynamics on the sphere”. *Journal of Computational Physics* 473 (2023), p. 111772.
- [9] C. J. Cotter, D. D. Holm, and P. E. Hydon. “Multisymplectic Formulation of Fluid Dynamics Using the Inverse Map”. *Proceedings: Mathematical, Physical and Engineering Sciences* 463.2086 (2007), pp. 2671–2687.
- [10] D. G. Ebin and J. Marsden. “Groups of diffeomorphisms and the motion of an incompressible fluid”. *Ann. of Math. (2)* 92 (1970), pp. 102–163.
- [11] C. Eckart and G. Young. “The approximation of one matrix by another of lower rank”. *Psychometrika* 1.3 (1936), pp. 211–218.
- [12] F. Flandoli, U. Pappaletta, and M. Viviani. “On the Infinite Dimension Limit of Invariant Measures and Solutions of Zeitlin’s 2D Euler Equations”. *Journal of Statistical Physics* 189.43 (2022).
- [13] A. Franken, M. Caliaro, P. Cifani, and B. J. Geurts. “Zeitlin truncation of a shallow water quasi-geostrophic model for planetary flow”. *Journal of Advances in Modeling Earth Systems* 16 (2024), pp. 1–16.
- [14] A. Franken, E. Luesink, S. Ephrati, and B. Geurts. *Casimir preserving numerical method for global multilayer geostrophic turbulence*. 2024. arXiv: [2409.05410](https://arxiv.org/abs/2409.05410).
- [15] I. Gallagher. “Mathematical analysis of a structure-preserving approximation of the bidimensional vorticity equation”. *Numer. Math.* 91.2 (2002), pp. 223–236.
- [16] E. S. Gawlik, P. Mullen, D. Pavlov, J. E. Marsden, and M. Desbrun. “Geometric, variational discretization of continuum theories”. *Phys. D* 240.21 (2011), pp. 1724–1760.
- [17] E. S. Gawlik and F. Gay-Balmaz. “A variational finite element discretization of compressible flow”. *Found. Comput. Math.* 21.4 (2021), pp. 961–1001.
- [18] E. Hairer, C. Lubich, and G. Wanner. *Geometric numerical integration*. Second. Vol. 31. Springer Series in Computational Mathematics. Springer-Verlag, Berlin, 2006.
- [19] J. Hoppe. “Diffeomorphism groups, quantization, and $SU(\infty)$ ”. *Internat. J. Modern Phys. A* 4.19 (1989), pp. 5235–5248.
- [20] J. Hoppe and S.-T. Yau. “Some properties of matrix harmonics on S^2 ”. *Comm. Math. Phys.* 195.1 (1998), pp. 67–77.
- [21] B. Kádár, I. Szyunyogh, and D. Dévényi. “On the Origin of Model Errors. Part II. Effects of the Spectral Discretization for Hamiltonian Systems”. *Időjárás. Quarterly J. Hungarian Meteorological Service* 102.2 (1998), pp. 71–107.
- [22] C. Lubich and I. V. Oseledets. “A projector-splitting integrator for dynamical low-rank approximation”. *BIT* 54.1 (2014), pp. 171–188.
- [23] K. Modin and M. Perrot. “Eulerian and Lagrangian stability in Zeitlin’s model of hydrodynamics”. *Comm. Math. Phys.* 405.8 (2024), Paper No. 177, 23.
- [24] K. Modin and M. Viviani. “Lie–Poisson methods for isospectral flows”. *Foundations of Computational Mathematics* 20.4 (2020), pp. 889–921.
- [25] K. Modin and M. Viviani. “A Casimir preserving scheme for long-time simulation of spherical ideal hydrodynamics”. *J. Fluid Mech.* 884 (2020), A22, 27.
- [26] K. Modin and M. Viviani. “Canonical scale separation in two-dimensional incompressible hydrodynamics”. *J. Fluid Mech.* 943 (2022), Paper No. A36, 22.
- [27] K. Modin and M. Viviani. *Two-dimensional fluids via matrix hydrodynamics*. 2024. arXiv: [2405.14282](https://arxiv.org/abs/2405.14282).
- [28] H. Munthe-Kaas. “Lie-Butcher theory for Runge-Kutta methods”. *BIT Numerical Mathematics* 35.4 (1995), pp. 572–587.
- [29] C. Pagliantini. “Dynamical reduced basis methods for Hamiltonian systems”. *Numer. Math.* 148.2 (2021), pp. 409–448.
- [30] D. Pavlov, P. Mullen, Y. Tong, E. Kanso, J. Marsden, and M. Desbrun. “Structure-preserving discretization of incompressible fluids”. *Physica D: Nonlinear Phenomena* 240.6 (2011), pp. 443–458.
- [31] Y.-D. Wu and X.-Q. Liu. “A short note on the Frobenius norm of the commutator”. *Math Notes* 87 (2010), pp. 903–907.
- [32] V. Zeitlin. “Self-consistent finite-mode approximations for the hydrodynamics of an incompressible fluid on nonrotating and rotating spheres”. *Physical review letters* 93.26 (2004), p. 264501.
- [33] V. Zeitlin. “Finite-mode analogs of 2D ideal hydrodynamics: coadjoint orbits and local canonical structure”. *Phys. D* 49.3 (1991), pp. 353–362.